ABILITY AND LIMITATIONS OF GENERAL CIRCULATION MODELS TO SIMULATE CLIMATE AND CLIMATE VARIABILITY

J. Shukla
Goddard Laboratory for Atmospheric Sciences
NASA/Goddard Space Flight Center, Greenbelt, MD 20771, USA

1. INTRODUCTION

Since the publication of the proceedings of the JOC Study Conference on climate models: Performance, Intercomparison and Sensitivity Studies, held in Washington, 3-7 April 1978 (GARP Publications Series No. 22), several journal papers and scientific reports have appeared describing the results of simulation of mean climate and climate variability. It is beyond the scope of this position paper to review all such papers. We have therefore chosen only a few selected papers whose contents will be summarized here. For a description of the simulation of the mean climate we have summarized the results of Shukla, et al. (1981a) for the climate variability the results of Manabe and Hahn (1981), Charney and Shukla (1981) and Lau (1981). Choice of these papers was based at least in part on convenience and familarity; however, since these papers were published recently, it is anticipated that they would provide a fair representation of the abilities and limitations of the current GCMs.

1.1 The Mean Climate

The time averaged circulation or the 'mean climate' of the atmosphere is determined by a balance between the radiative forcing (shortwave and longwave radiation), the stationary forcings at the earth's surfce (mountains, land-ocean-ice distribution) and the dynamical fluxes of heat, momentum and moisture. For a realistic simulation of the mean climate it is therefore necessary to calculate each of the three components accurately. Calculation of accurate radiative fluxes requires accurate vertical profiles of temperature, moisture, 0_3, CO_2, other trace gases and aerosols, and an accurate treatment of cloud-radiation interaction for space-time variable clouds. To accurately calculate the stationary forcings at the earth's surface, it is necessary to model correctly the thermal and mechanical effects of mountains and the heat and moisture fluxes across land-air, sea-air, snow-air and ice-air interfaces. And finally, an accurate calculation of the dynamical fluxes requires the simulation of the correct amplitudes and phases of stationary and transient eddies, their growth and decay, and their interactions among themselves and with the mean circulation. One of the primary objectives of general circulation modelling groups has been to simulate the mean climate realistically by incorporating the above complex processes in a single model. For a variety of reasons it has not been possible to treat all the physical-dynamical processes discussed above with uniform degree of sophistication. Some processes are treated in great detail whereas other processes are parameterized to a high degree of simplifcation. Due to the large number of parameters and processes it has not been possible in all cases to conduct extensive integrations to determine the appropriate levels of complexity for parameterizations of physical processes. It is therefore very difficult to compare the models with each other; what is most convenient is to compare each model individually with observations.

The discussions in the present paper will be confined to comparisons with observations and no attempt will be made to describe the model sensitivity to external forcings, parameterizations of physical processes, chemical composition, etc.

1.2 The Interannual Variability

The interannual variability of the time mean or transient circulation can be considered to consist of two parts: the part due to the internal dynamics with prescribed seasonally varying boundary forcings, and the part due to the interannual variability of boundary forcings themselves. The boundary conditions of sea surface temperature (SST), soil moisture, snow, sea ice, etc., can be hypothetically prescribed to have their mean seasonal variation, and GCMs can be integrated for several years to calculate the interannual variability due to internal dynamics. Similarly GCMs can be integrated with time varying (interannually as well as seasonally) boundary forcings to determine the total interannual variability due to the combined effects of internal dynamics and boundary forcings. To our knowledge, none of the above two integrations have been performed with any large complex GCM for 10 years or more. One model simulation, that of Manabe and Hahn (1981), would seem to be just such an integration, yet it falls in neither category. In their model, Manabe and Hahn prescribed the seasonally varying (but not interannually varying) SST but allowed the soil moisture and snow cover to vary interannually as determined by the model parameterizations. We shall come back to the results of Manabe and Hahn in Section 4.

The ability and limitations of the GCMs to simulate climate and climate variability will be discussed for tropics and mid-latitudes, in the following broad categories:

a) Mean climate
b) Space-time fluctuations within a season
c) Interannual variability of monthly, seasonal and annual means
d) Interannual variability of intra-seasonal space-time fluctuations.

The main emphasis of this paper was supposed to be the simulation of tropical variability. Since tropical and mid-latitude variability may be related and since it was difficult to isolate the tropics in the results of global GCMs, we have chosen to describe the global circulation and its variability with particular emphasis on tropics. For additional discussion of mid-latitude simulations, see Gilchrist (1982). For a more comprehensive discussion of simulation of tropical mean and transient circulations by GFDL models, the reader is referred to pioneering works of Manabe and his colleagues (Manabe and Smagorinsky, 1967; Manabe et al., 1970; Manabe et al., 1974; Hayashi, 1974; Hayashi and Golder, 1980).

Section 2 presents the results for mean climate, Section 3 for intra-seasonal space-time fluctuations, Section 4 for interannual variability of monthly and seasonal means, and Section 5 for interannual variability of intra-seasonal fluctuations. Section 6 gives a summary and the conclusions.

2. MEAN CLIMATE

We present here a summary of simulation results from the GLAS (Gloddard Laboratory for Atmospheric Sciences) climate model which has been extensively described in Shukla et al. (1981a).

Sea level pressure: Figures 1a and 1c show the observed 16 year mean sea level pressure for January and July reproduced from Godbole and Shukla (1981), and Figures 1b and 1d show the model simulated mean sea level pressure for the single February and July respectively. For February, the simulation of the prominent Northern Hemispheric circulation features, such as the Aleutian and Icelandic lows, is fairly realistic, but the discrepancy in the structure and intensity of the Siberian high is too large to be accounted for

(a)

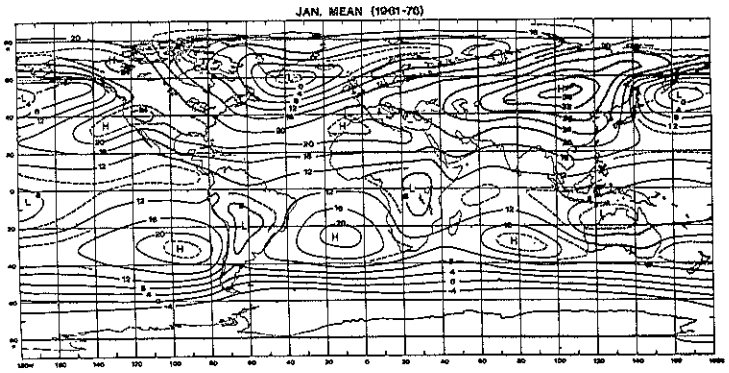

(c)

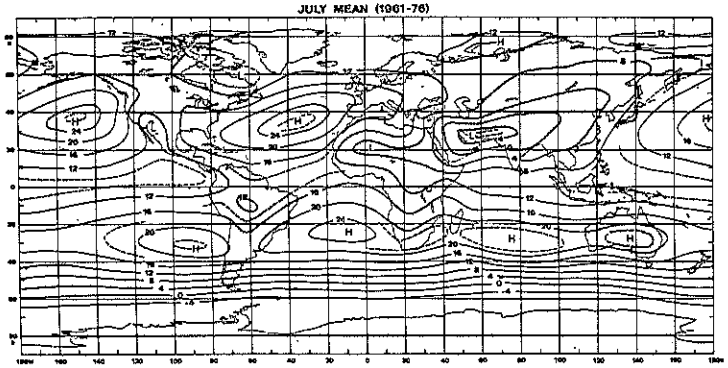

(b)

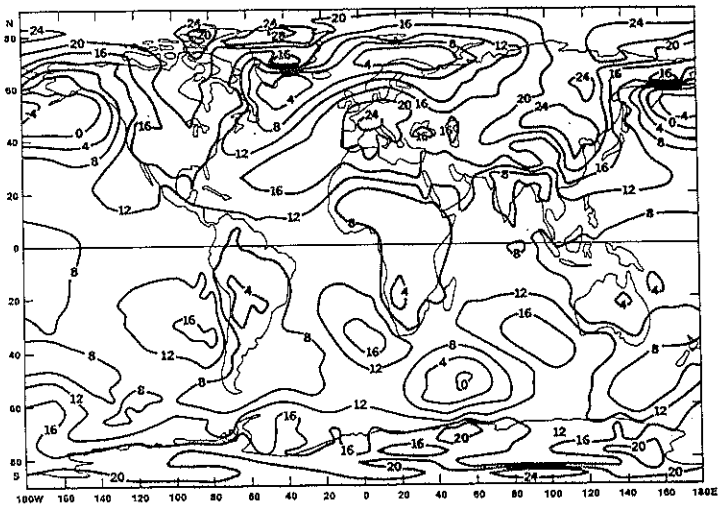

(d)

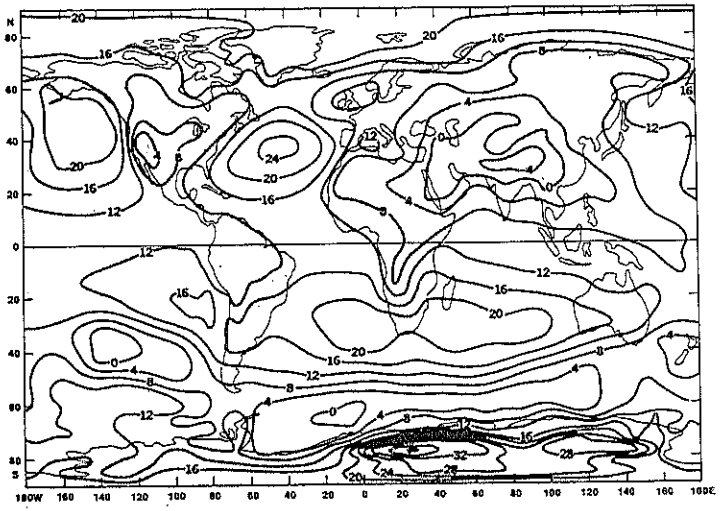

Figure 1 Mean sea level pressure (-1000 mb): (a) Observed January (Godbole and Shukla, 1981), (b) GCM February, (c) Observed July (Godbole and Shukla, 1981), (d) GCM July.

by interannual variability or by differences between January and February. The most serious deficiency of the simulated field is in the Southern Hemisphere, south of 60°S, where the simulated field shows a large eddy structure and the observed field is zonally uniform. For July the high pressure cell over the North Atlantic and the monsoon low are well simulated, but the orientation of North Pacific high is not as observed. The subtropical high pressure cells in the Southern Hemisphere are well simulated over the Indian Ocean, Atlantic Ocean and the eastern Pacific but not over Australia. For summer and winter both the models show a common deficiency of distinct non zonal isobar configurations in the Southern Hemispheric mid-to-high latitudes.

Geopotential height: Figure 2 shows the observed and simulated geopotential height field at 200 mb. For February, the simulated trough over northeast USA and eastern Canada, the ridge over the eastern Atlantic, the jet stream over Japan and the anticyclonic circulation over the tropics are quite realistic. However, the ridge over the west coast of the USA is displaced to the east, and the Southern Hemisphere mid-latitudes show more eddy structure than is observed. For July, there are several deficiencies in the simulated field. Large amplitude short waves are seen over North America and adjacent Pacific Ocean, and the geopotential heights in the tropical belt are higher by about 200 gpm than climatology.

The surface circulation during July and the upper level circulation during January are, in general, better simulated than the surface circulation during winter and the upper level circulation during summer.

Zonal wind and temperature: Figure 3 shows the observed and simulated zonal wind and zonally averaged temperature. For February, the locations of the strongest zonal wind maxima in both hemispheres are well simulated. The most conspicuous deficiency is the absence of the closed maximum near 200 mb which is seen in the observed zonal winds. This is related to the very low model temperatures in the upper troposphere polar regions. The model simulated tropical atmosphere is considerably warmer than the observations. Cooling near the poles and the large zonal winds near the upper boundary have been one of the common deficiency of GCMs and their precise cause is yet to be determined.

Stationary wave variance: Figure 4 shows the observed and simulated variance around a latitude circle of the winter and summer mean stationary geopotential height summed over the planetary waves (wavenumber 1-4). The latitudinal and height distributions of the simulated variance are in good agreement with the observations for both seasons. The observed decrease of variance above 300 mb is not simulated and this is probably related to the low polar temperatures and strong zonal winds at the upper levels.

Surface winds and ITCZ: Figures 5 and 6 show the observed and simulated surface winds reported in the modelling study of Halem et al. (1979). The corresponding maps from Shukla et al. (1981a) are quite similar to these. The observed fields are from Mintz and Dean (1952). The agreement between the observed and the simulated ITCZ is very good, especially with regard to the longitudinal variation of the ITCZ. The structure and locations of anticyclonic centres are also well simulated. The seasonal reversal from northeasterly winds during winter to southwesterly winds during summer over the north Indian Ocean is correctly simulated by the model. The main discrepancy in the latitudinal location of the ITCZ occurs during winter over the eastern part of the Pacific and over the Indian Ocean.

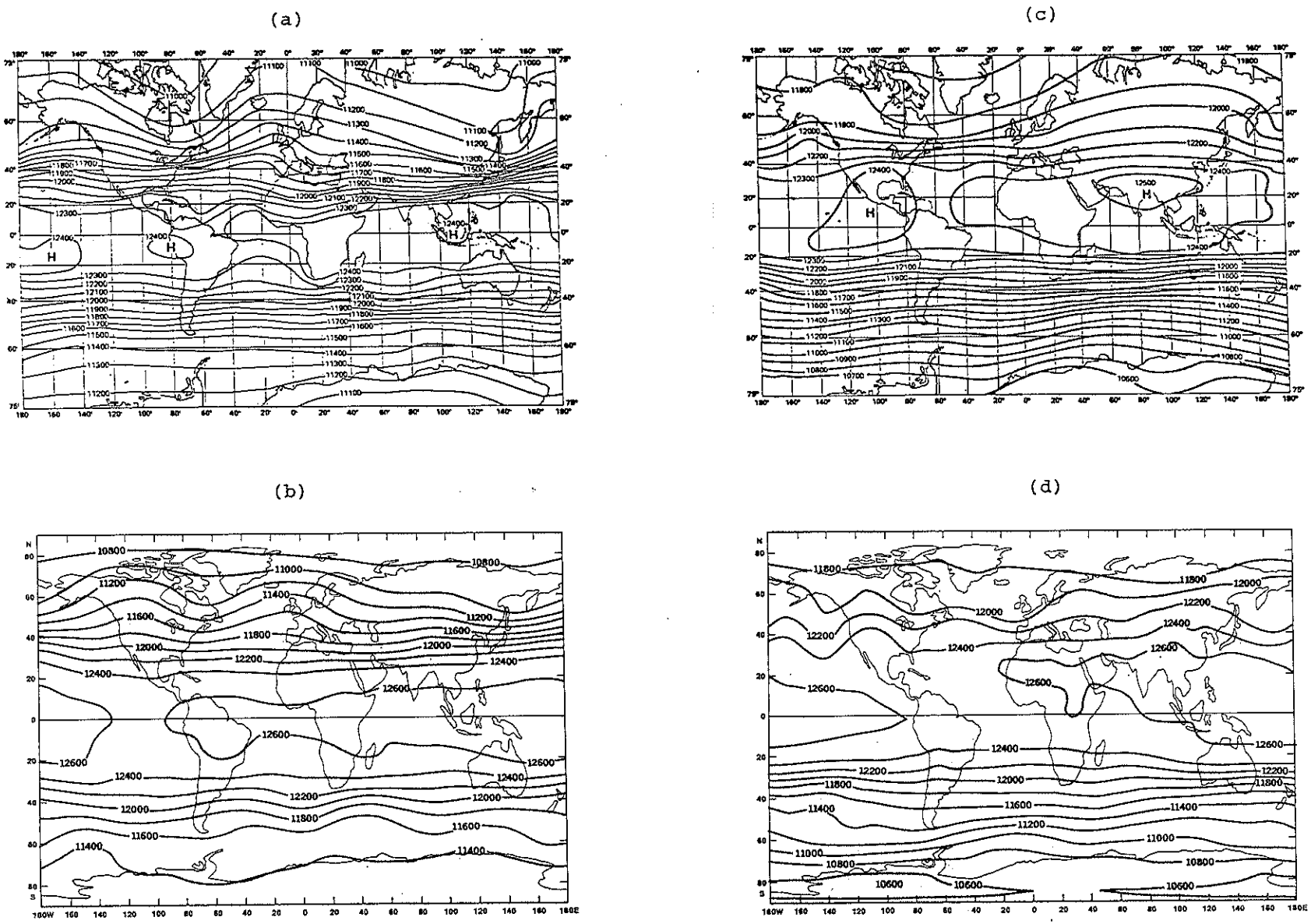

Figure 2 Mean geopotential height (gpm) at 200 mb: (a) Observed December, January and February (Crutcher and Davis, 1969), (b) GCM February, (c) Observed June, July and August (Crutcher and Davis, 1969), (d) GCM July.

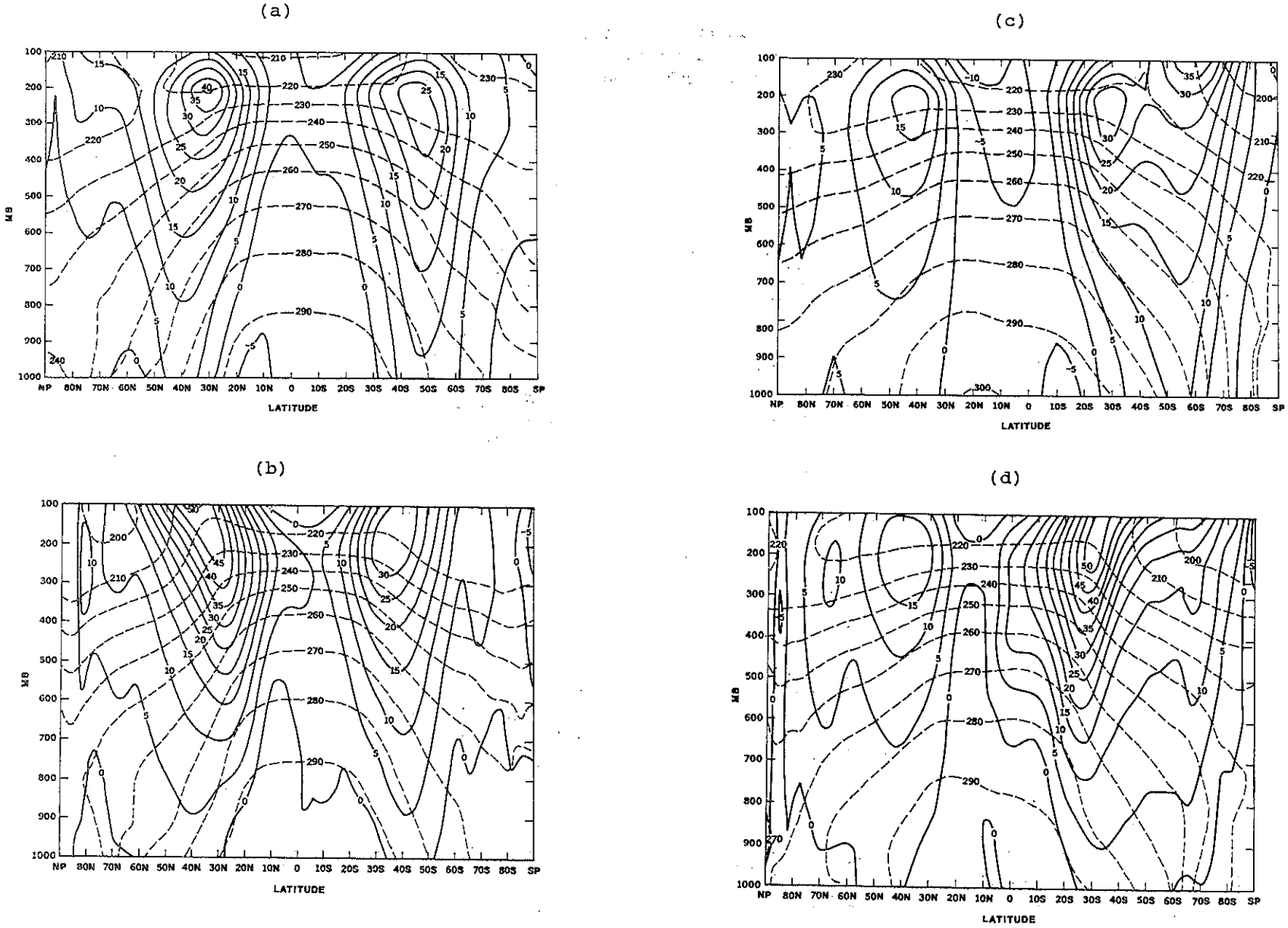

Figure 3 Zonally averaged zonal wind (ms^{-1}, solid lines) and temperature (°K, dashed lines): (a) observed February, 1979, (b) GCM February, (c) observed July, 1979, (d) GCM July.

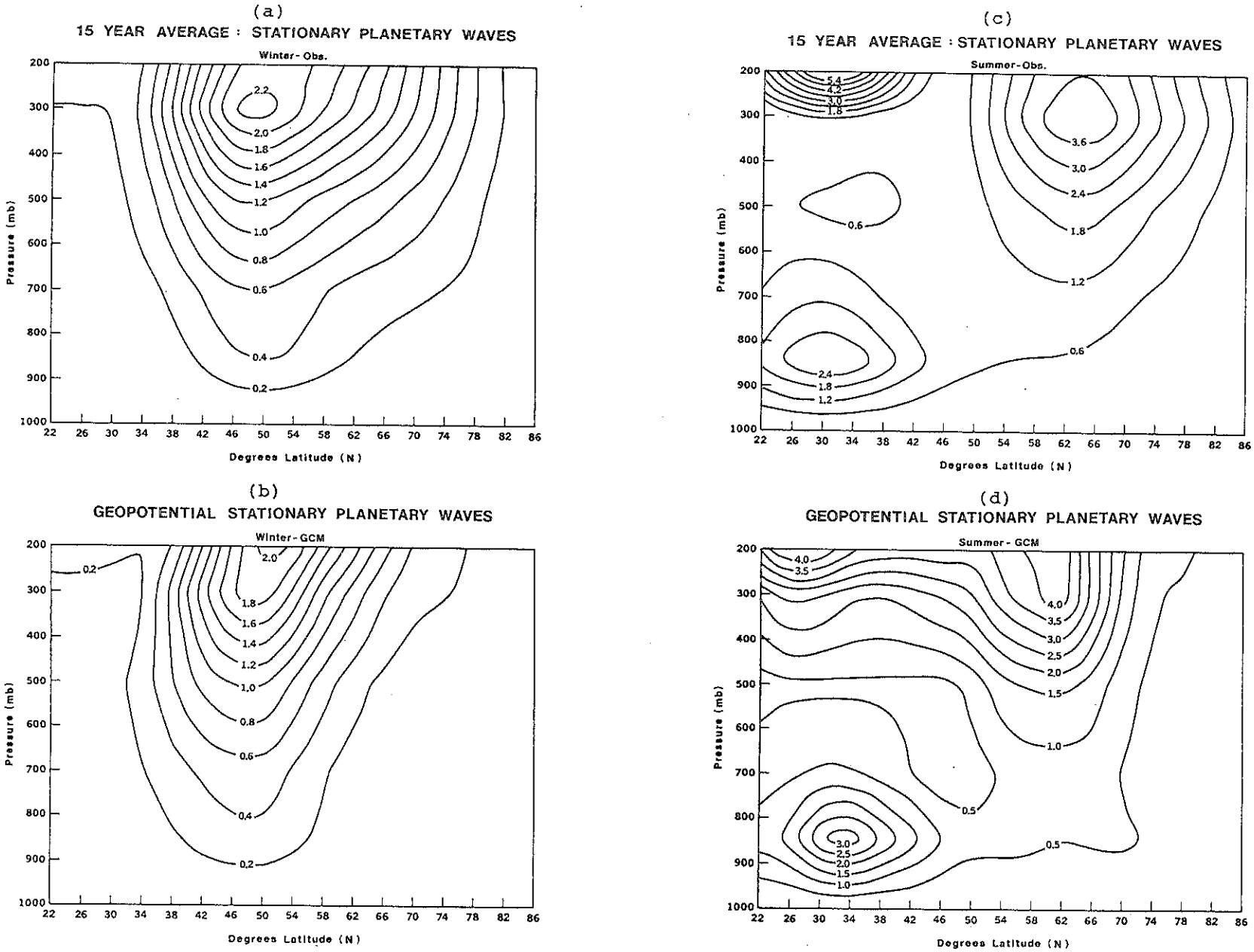

Figure 4 Stationary planetary wave variance of the geopotential height in the Northern Hemisphere: (a) observed winter (units of 10^4 m^2), (b) GCM winter (units of 10^4 m^2), (c) observed summer (units of 10^3 m^2), (d) GCM summer (units of 10^3 m^2).

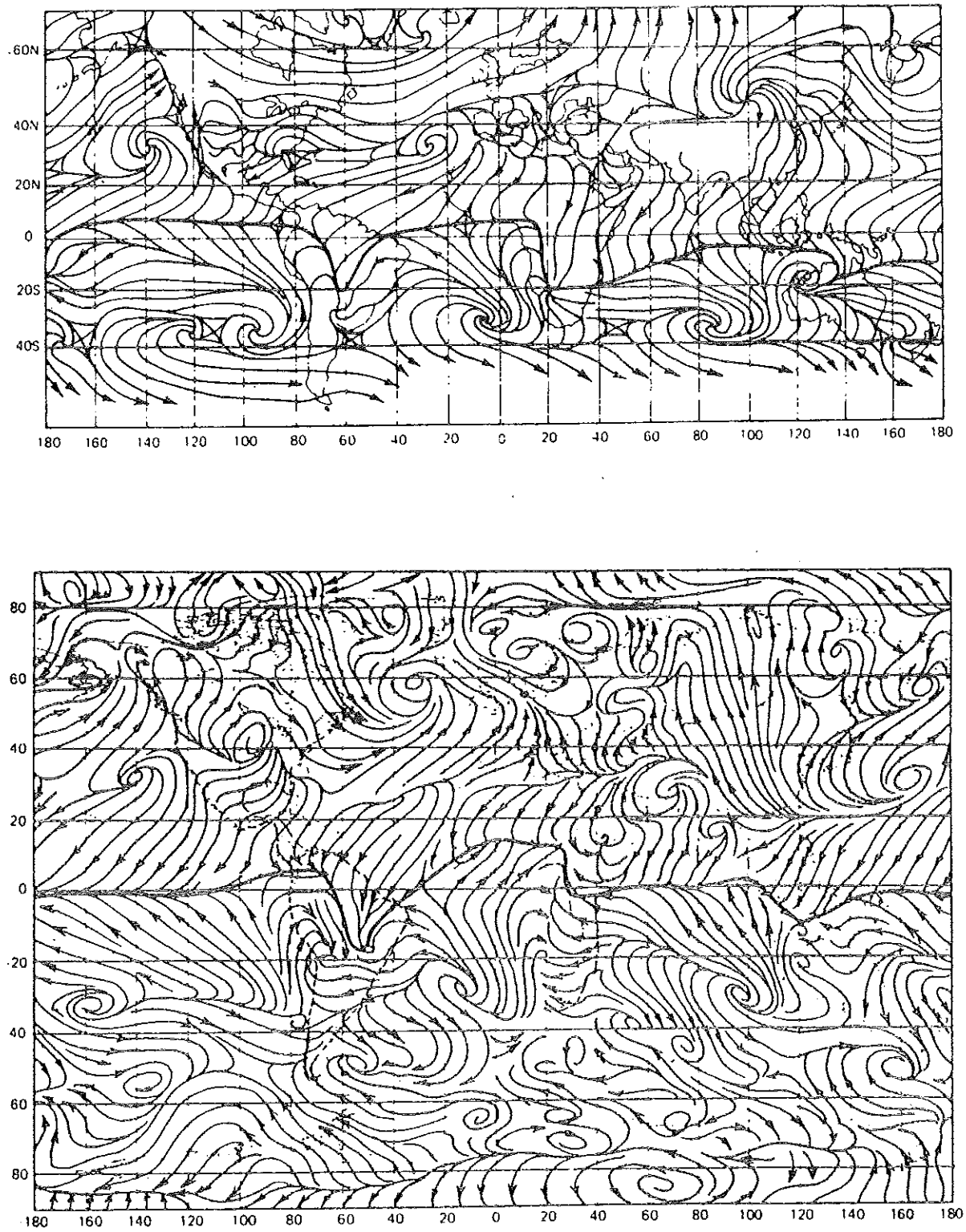

Figure 5 Streamlines at earth surface: (a) observed January (Mintz and Dean, 1952), (b) GCM February (Halem et al., 1979).

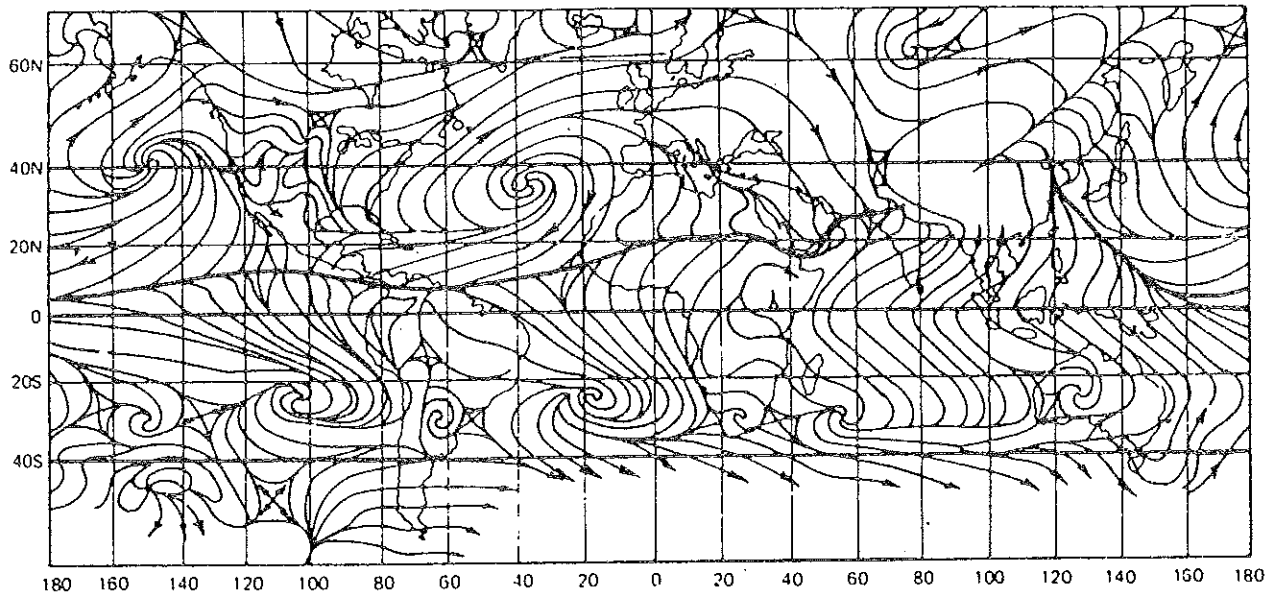

(a)

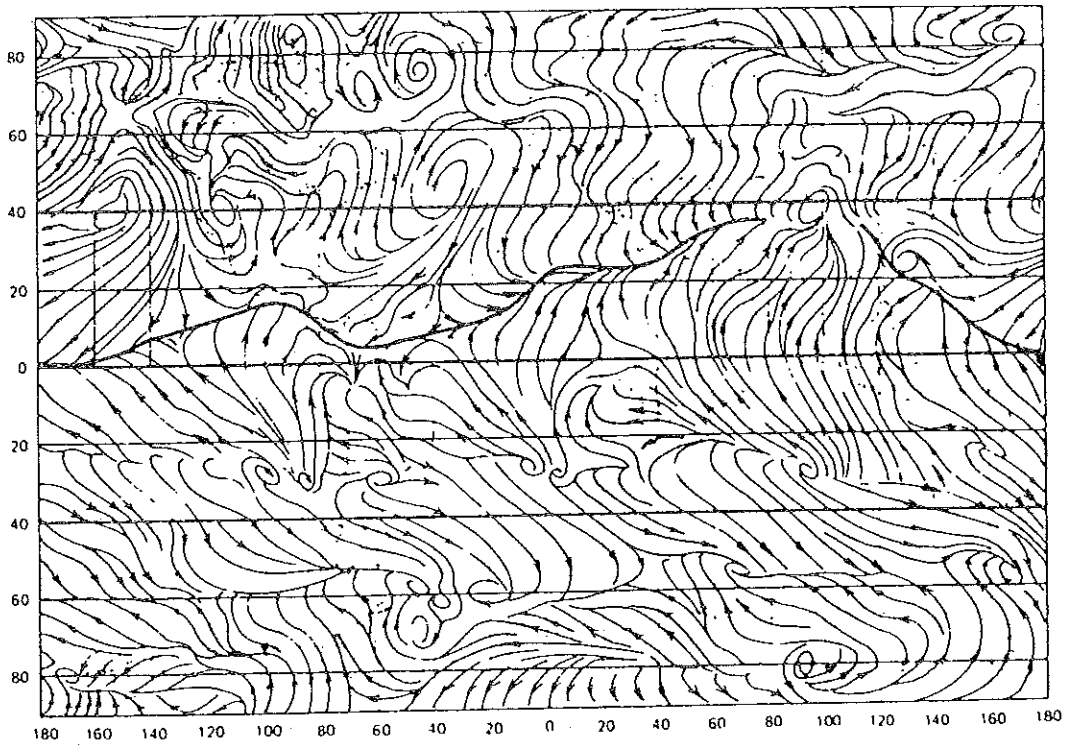

(b)

Figure 6 Streamlines at earth surface: (a) observed July (Mintz and Dean, 1952), (b) GCM February (Halem et al., 1979)

Rainfall: Figures 7 and 8 show the observed (from Jaeger, 1976) and simulated monthly mean rainfall for winter and summer respectively. Considering the large variability of rainfall and the uncertainty in the observations, the agreement between the simulated and the observed rainfall patterns is very good. Areas of very large and very small rainfall are well reproduced. The most obvious discrepancies are the excessive February precipitation over the Tibetain Plateau and the overprediction of July rainfall over eastern North America. Partition of the total precipitation between large scale and convective (cumulus) precipitation (not shown) showed that in both seasons cumulus precipitation dominates in the tropics, and large scale precipitation in higher latitudes.

Upper level flow: The simulation of the 200 mb flow (now shown) by Shukla et al (1981a) is in good agreement with the observations. For February, the locations and the intensities of the jet streams in both hemispheres are well simulated, although the simulated jet stream speeds were stronger than the observations for 1979, to which they are compared in Shukla et al.

Manabe et al. (1979) have presented simulation results from spectral models with 15, 21 and 30 wavenumbers. They found that the increase in spectral resolution improved the simulation of tropical rainbelts and subtropical dry zones. An example of one of the better simulations of the upper level flow with a 30 wavenumber spectral model is shown in Figure 9, reproduced from Hayahsi (1980). The large scale features of the Tibetan and Mexican highs, the mid-Pacific and mid-Atlantic troughs, and the easterly jet off southern Asia are better simulated in the spectral model than in the grid model. A detailed discussion of the relative merits of grid point and spectral models is beyond the scope of this paper.

3. SPACE-TIME FLUCTUATIONS WITHIN A SEASON

For GCMs to be a useful tool for sensitivity and predictability studies, it is necessary that they not only simulate accurately the time averaged circulation but also the different components of the transient circulations. We present here the simulation of low frequency planetary wave variance and the local band-pass variance from the GLAS climate model and the GFDL grid point model. In Section 3.1 we describe the model's ability to simulate blocking situations.

Low Frequency Planetary Wave (LFPW) variance: The LFPWs consist of wave-numbers 1-4 with periods of 7.5 to 90 days. Figure 10 shows the observed and simulated latitude-height structure of the LFPWs. There is general agreement in the overall structure for both winter and summer seasons. The discrepancy near the upper level is same as in the earlier fields, and in addition, the model variances are somewhat too small.

Band-pass variance: Figure 11 shows the observed and simulated local band-pass filtered variance of the 500 mb geopotential height in the Northern Hemisphere for the winter season. The band-pass variance is defined as the spatially local root mean square (RMS) deviation in time for fluctuations of 2.5 to 6 days. The band-pass variance is related to the frequency, intensity, growth and decay of cyclonic storms and indiates the location of "storm tracks" (Blackmon et al, 1977). The observed and simulated band-pass RMS for winter show excellent agreement in terms of both the location and the strength of the major areas of cyclonic activity in the north Central Pacific and western Atlantic. For summer (not shown) the Atlantic maximum has been realistically simulated, both with respect to position and to magnitude, but the simulated Pacific maximum is too weak and is located too far to the west.

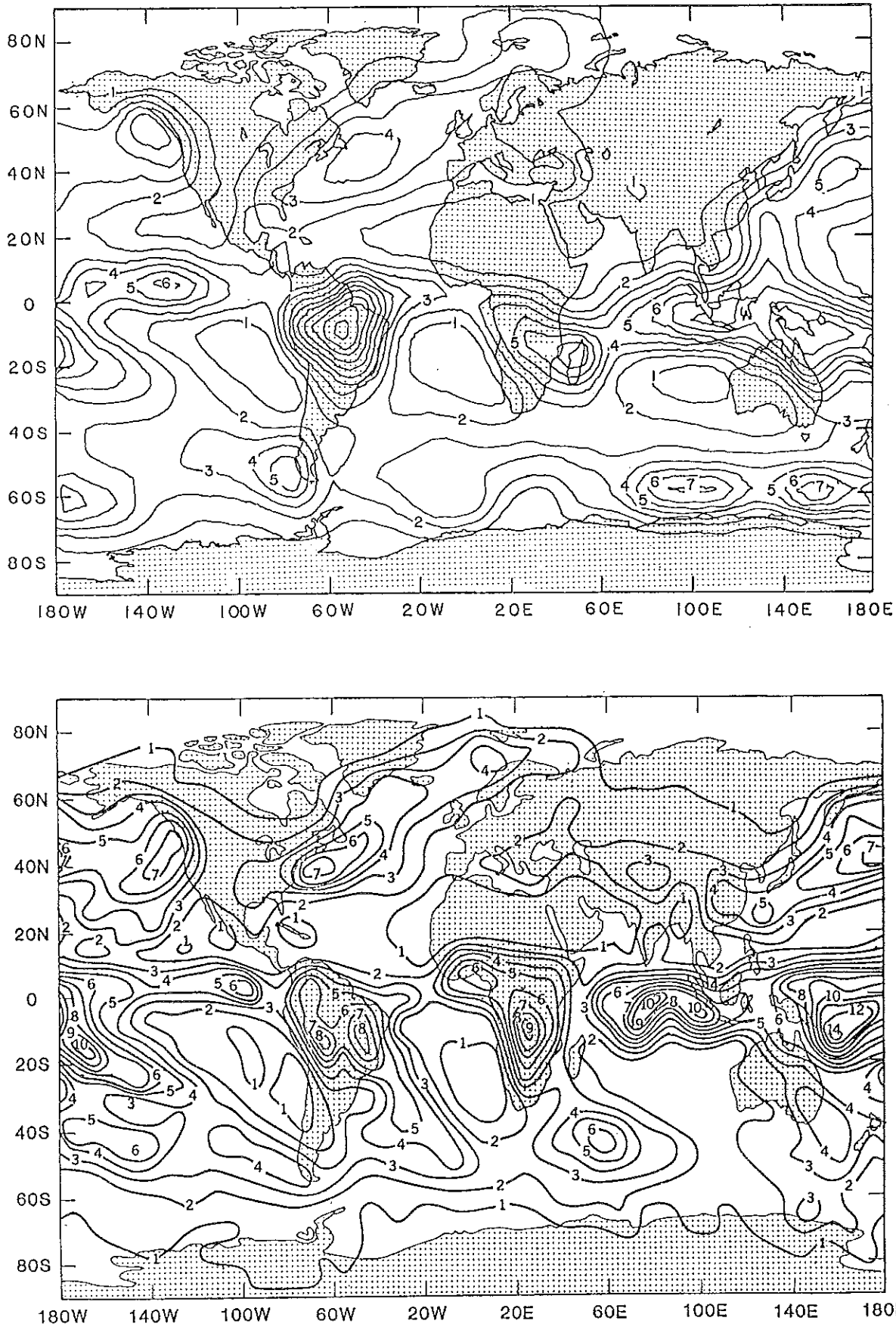

Figure 7 Precipitation (mm day^{-1}): (a) observed February (Jaeger, 1976), (b) GCM February.

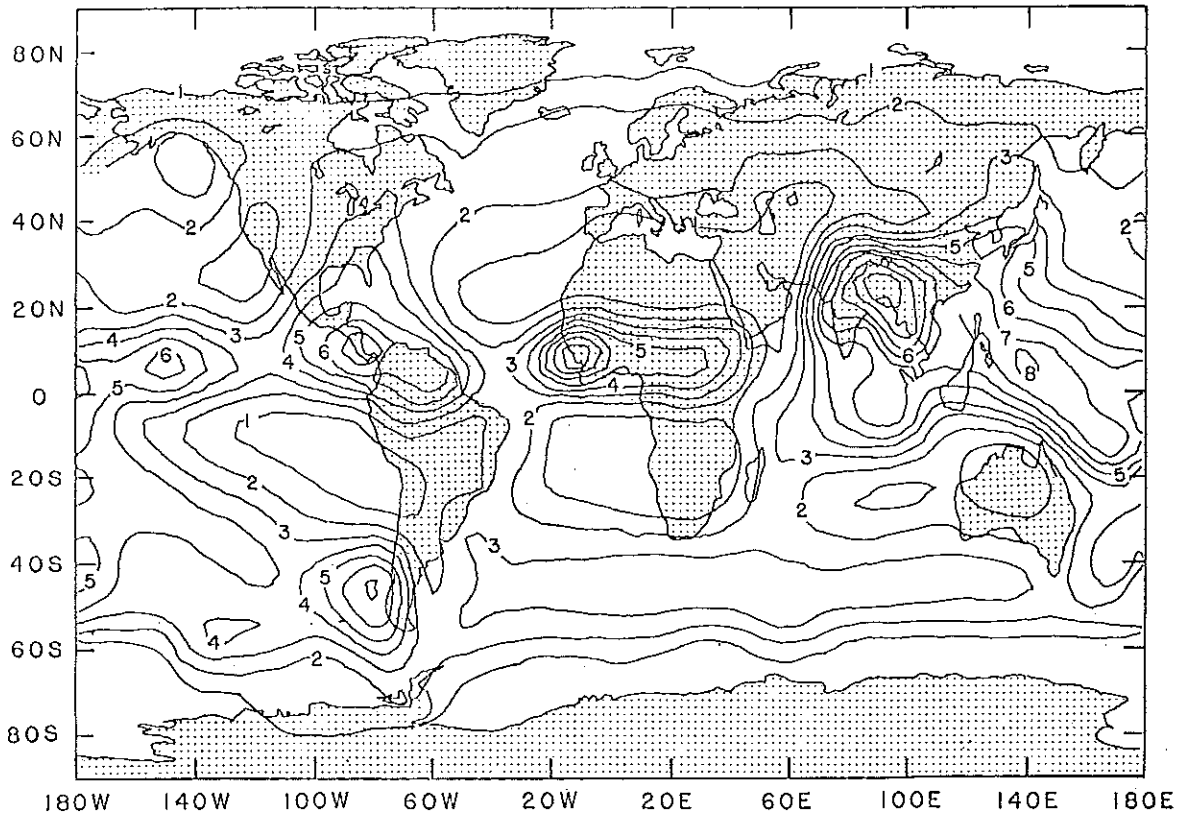
80N
60N
40N
20N
0
20S
40S
60S
80S
180W
140W
100W
60W
20W
20E
60E
100E
140E
180E

(a)

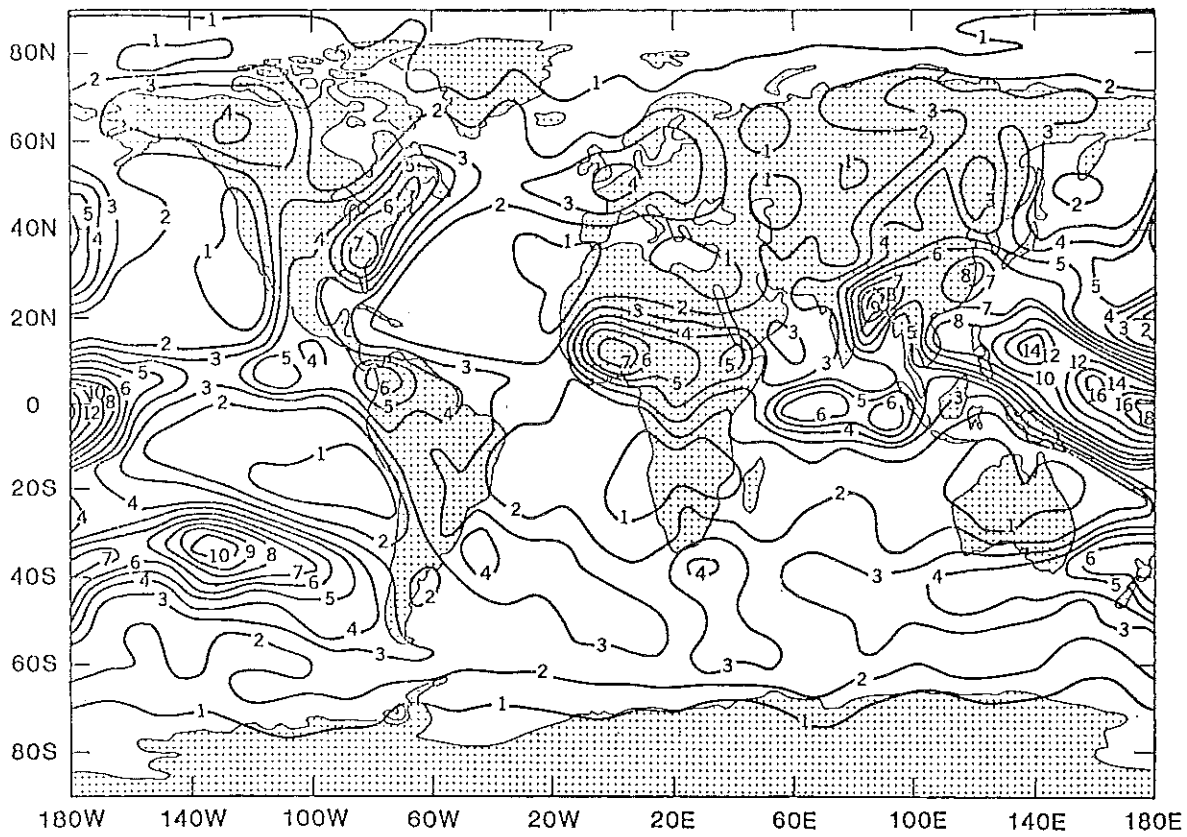
80N
60N
40N
20N
0
20S
40S
60S
80S
180W
140W
100W
60W
20W
20E
60E
100E
140E
180E

(b)

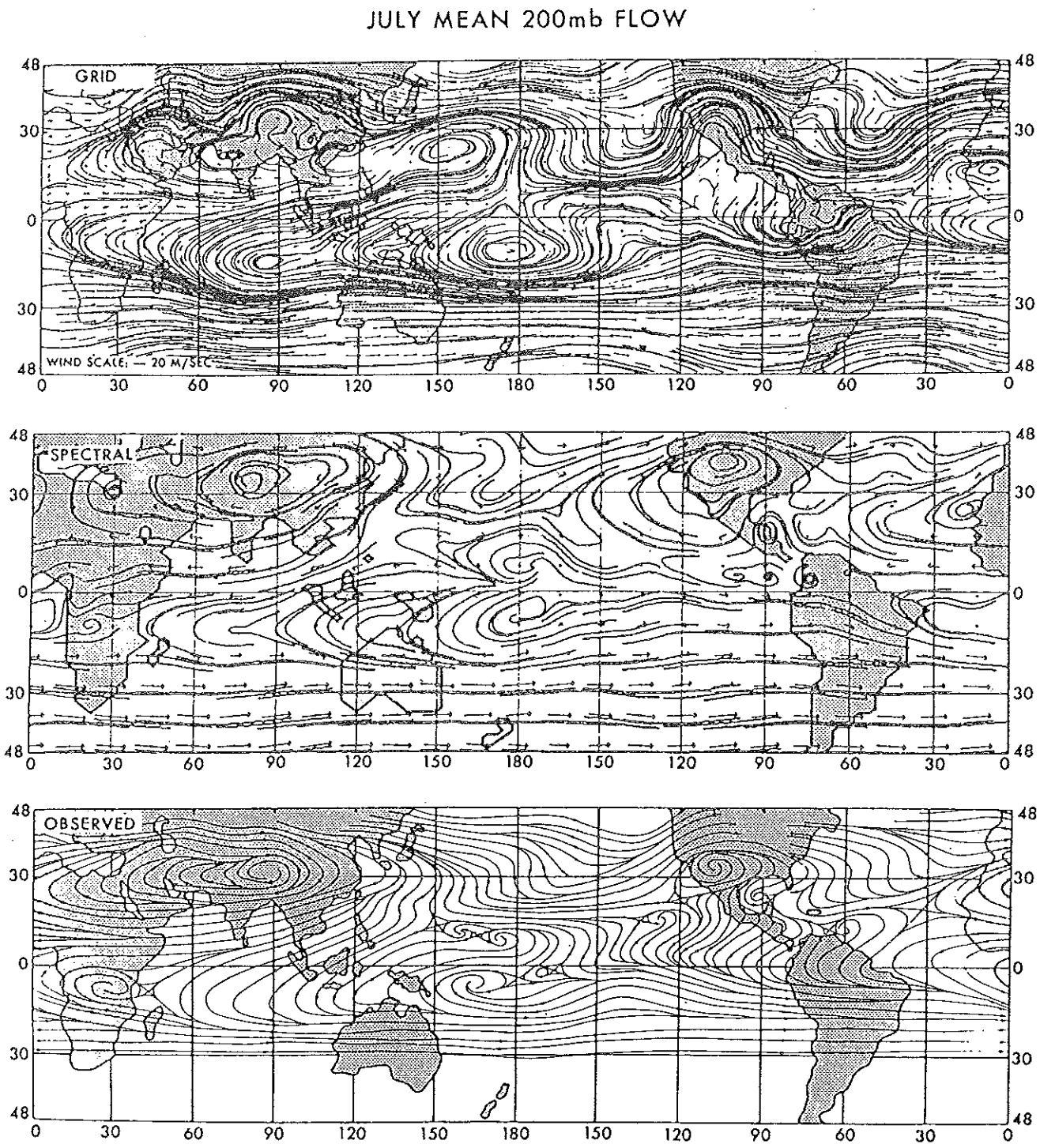

Figure 9 July mean streamlines: (top) computed at 190 mb (grid model, Manabe et al., 1974), (middle) computed at 205 mb (spectral model, Manabe et al., 1979), (bottom) observed at 200 mb (Sadler, 1975).

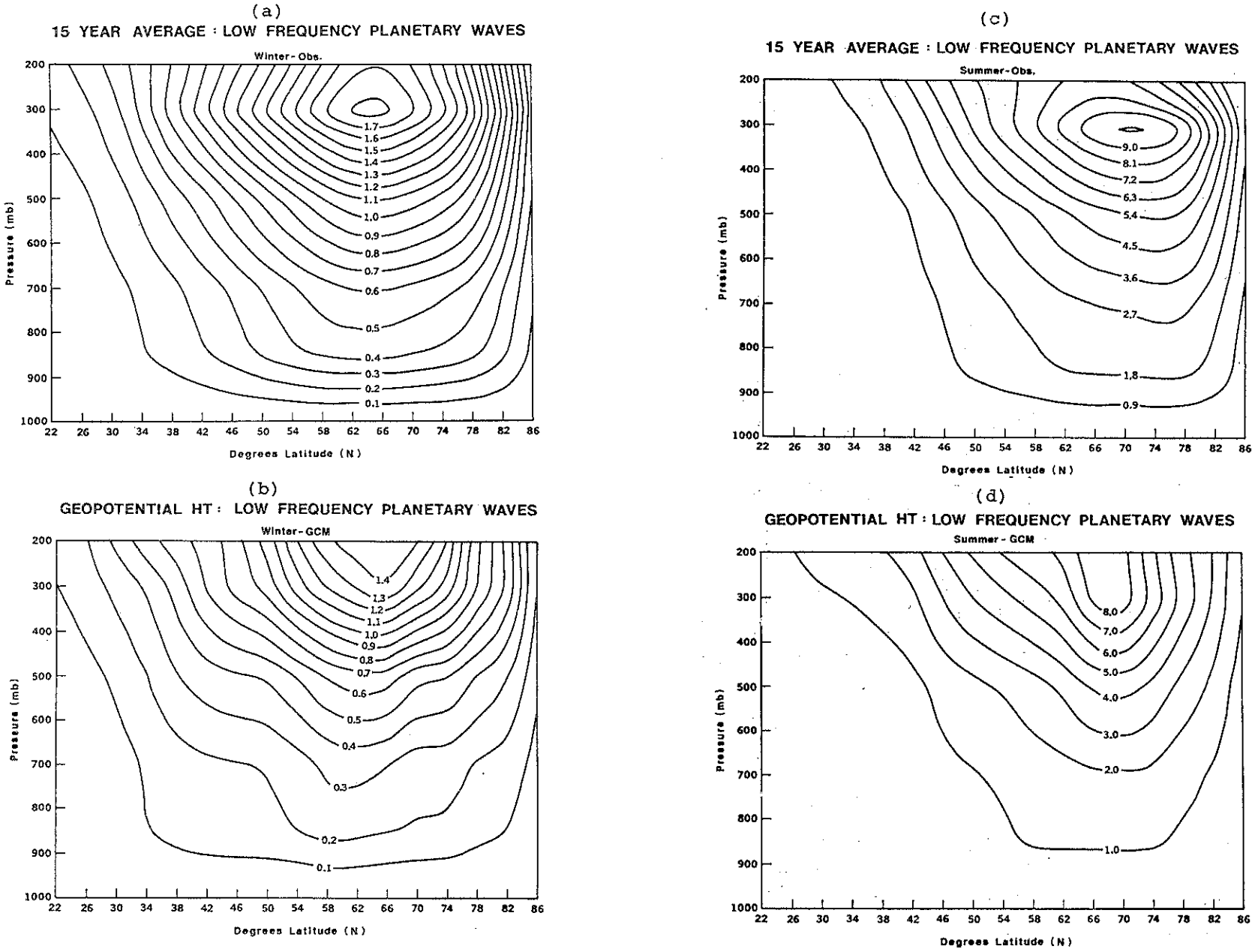

Figure 10 Geopotential height variance in low-frequency planetary waves in the Northern Hemisphere: (a) observed winter (in units of 10^4 m^2, contour interval is .1 x 10^4 m^2), (b) GCM winter (in units of 10^4 m^2, contour interval is .1 x 10^4 m^2), (c) observed summer (in units of 10^3 m^2, contour interval is .9 x 10^3 m^2), (d) GCM summer (in units of 10^3 m^2, contour interval is 1.0 x 10^3 m^2).

(a)

(b)

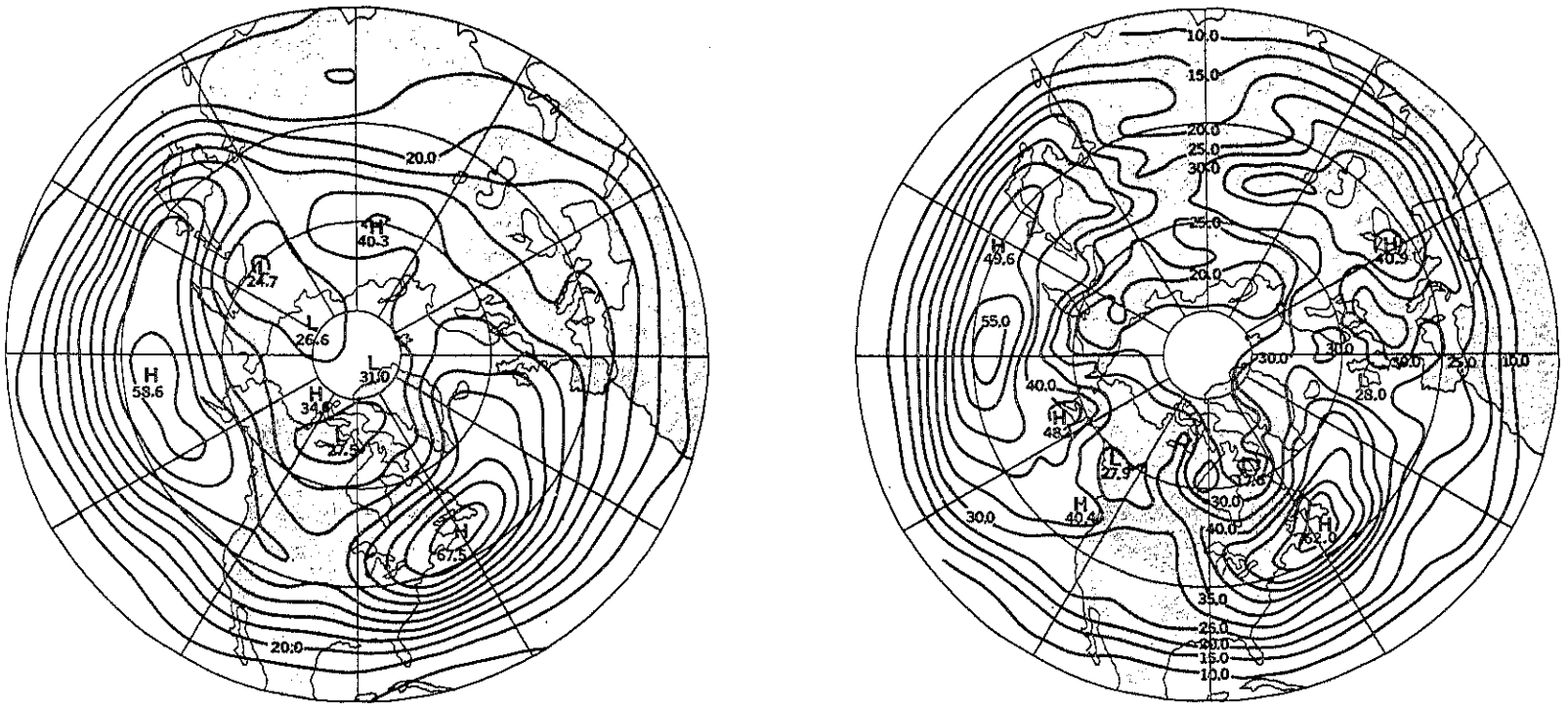

Figure 11 RMS deviation of the winter 500 mb band-pass geopotential height field in the Northern Hemisphere, units of m (contour interval is 5 m): (a) observed winter, (b) GCM winter.

Blackmon and Lau (1980) have analyzed the variance and co-variance of band-pass filtered and low-pass filtered data from simulations of a GFDL model earlier described by Manabe et al (1974). They found good agreement between the observations and the model simulated location and intensity of storm tracks, vertical structure of the disturbances, and transport of heat and potential vorticity by transient eddies. The total RMS and the low-pass filtered RMS of the 500 mb height were weaker in the model simulations compared to the observations. In the end of the same paper, Blackmon and Lau (1980) have also presented a brief summary of circulation statistics from the simulation of a second generation NCAR GCM and noted that in general the model simulates accurately the geographical structures of the variance fields, but that the magnitude and vertical structure are not well simulated.

Based on the results of Blackmon and Lau (1980), and Shukla et al. (1981a) the following general comments can be made about the ability of these GCMs to simulate mid-latitude intra-seasonal variability.

a) GCMs show a remarkable degree of success in simulating the geographic location, intensity and life cycle of synoptic scale disturbance. This is inferred from the similarities in observed and model simulated band-pass filtered height variances. The geographic locations of the storm tracks in relation to mean field structures are also well simulated.

b) GCMs do not simulate as well the low-pass filtered variance. The amplitudes are less in every model and sometimes even the geographical locations are not well simulated. Since the maxima in low-pass variance are coincident with the maxima in low-pass variance are coincident with the maxima in the frequency of blocking in all seasons (Shukla and Mo, 1981; Dole, 1982) it may be conjectured that the models do not simulate the amplitude, alocation and duration of observed blocking events.

3.1 Simulation of Blocking

The mid-latitude atmospheric flow pattern is occasionally dominated by quasi-persistent features whose time scale is larger than the life cycle of individual storms but shorter than the length of a season. These features, generally referred to as blocking, are of great importance to medium range and monthly prediction. Shukla and Mo (1981) and Dole (1982) have examined the geographical and seasonal occurrences of persistent anomalies in the geopotential height field over the Northern Hemisphere. They found that large positive anomalies (>100 - 200 m) have tendency to persist for 7-10 days at three distinctly different geographical locations: in the Pacific to the west of the Rockies, in the Atlantic to the west of the Alps, and in the Scandinavian mountain ranges and overland to the west of Ural mountains of the USSR. The local structure of blocking in all three regions is very similar and these preferred locations do not change with season. Similar analysis (i.e. using similar duration and intensity criteria) for long term integrations of GCMs is not available for comparison with the observations. This could readily be done for the simulations of Manabe and Hahn (1981).

A preliminary analysis of climatology of blocking in the GLAS climate model is presented by Shukla et al. (1981b). They examined 17 winter and 7 summer short term simulations to determine the frequency and geographical locations of the model simulated blocking events. A blocking event was identified if at any grid point the 500 mb geopotential height anomaly (departure from the mean seasonal cycle) of 100 gpm or more persisted for 7 days or

more. It was found that the geographical locations of the frequency of maximum blocking events were not in good agreement with observed locations. The model underestimated the intensity of blocking ridges. Several blocking type configurations appeared but they did not persist with amplified magnitude. Chen and Shukla (1982) have analyzed a case of strong blocking situation, the strongest simulated by the GLAS climate model, which occurred in a winter simulation with large SST anomalies in the northern Pacific as observed during January 1977. Mansfield (1981) has examined the blocking situations in the British Meteorological Office GCM.

The general conclusion based on examination of several model simulations is that the GCMs do not simulate the location, intensity and duration of blocking events. An exception is found in some recent perpetual winter simulations by the NCAR model (Blackmon, personal communication) where the model tends to overpredict the strength and duration of the blocking events. We can list several possible reasons for inadequate simulations of blocking events.

a) Resolution: If the maintenance of the blocks were due to interactions between the large scale circulation and small scale waves, and if the model resolutions were not adequate to resolve the latter and their interactions with the former, it could be suggested that the inadequate resolution is one of the causes for unrealistic simulation. Examination of blocking in high resolution models can shed further light on this matter.

b) Structure of the zonal flow: Tung and Lindzen (1979) have suggested that the vertical structure of zonal winds, especially at higher levels are very important in setting up stationary waves and blocking. Since most of the models do not simulate the zonal winds and temperatures at the higher levels, they may not produce realistic blocking events also. Incidentially, it should be noted that the NCAR model mentioned above which simulates large and persistent blocking events also shows very realistic simulation of the upper level zonal winds.

c) Diabatic heat sources: If some of the observed blocking events were either due to the influence of anomalous mid-latitude stationary thermal forcings (anomalies of SST, snow or sea ice, etc.) or due to tropical heat sources (anomalies of SST or soil moisture)m themodel simulations would not be able to simulate them because they use climatological boundary forcings. We do not understand the precise role of slowly varying boundary forcings in the generation and maintenance of blocking events. It seems reasonable to conjecture that the large scale quasi-stationary flow patterns may be initiated by stationary forcings but that the small scale waves and their interactions may be important for the maintenance of the blocks.

Even in the absence of quasi-stationary thermal forcings, blocks may be generated by interactions between fluctuating zonal winds and mountains (Charney and Devore, 1979; Charney and Straus, 1980; Charney, et al, 1981), and in this context lack of GCM's ability to simulte blocking can be attributed to inadequate treatment of interactions between the zonal flow and orography. The apparent regional nature of the blocking and locally amplified ridges could be due to the longitudinal variations of zonal flow (opinion of late Professor Charney) which are in turn caused by the longitudinal variations of diabatic heating. If GCMs were not able to simulate the heat sources and the asymmetric zonal flows, they would also be deficient in simulating the blocking events. We need more thorough analysis of blocking phenomena in GCM simulations.

Lau (1981) has shown that the so-called Pacific/North American pattern of monthly mean height anomalies is present in the simulation without SST anomalies. This does not necessarily mean that the SST anomalies are not important for blocking because the Pacific/North American pattern should not be considered as blocking. Gutzler (personal communication) has shown that the Pacific North American pattern can be found even if all the days identified as blocking were removed from the data set before the calculations for the pattern were made.

4. INTERANNUAL VARIABILITY OF MONTHLY, SEASONAL AND ANNUAL MEANS

Manabe and Hahn (1981) have presented the results of a simulation of atmospheric variability from the last 15 years of a 17.75 year integration of the GFDL spectral climate model. The description of the model and simulation of mean fields is given in Manabe et al. (1979). Sea surface temperature, cloud amounts, insolation and ozone are prescribed for each calendar day of the year and have no interannual variability; therefore the simulated interannual variability is mainly due to internal dynamics and changes in snow cover and soil moisture. The same model simulation has been studied by Lau (1981) to study recurrent meteorological anomalies. Major conclusions of these papers and related remarks can be summarized as follows:

a) The geographical stucture of the simulated variability of daily and monthly means is in good agreement with the observations. The magnitude of the variability is systematically underestimated in the tropics and is either comparable to or less than is observed in the middle latitudes. In the regions of systematic underestimation of simulated sea level pressure, daily and monthly variability is overestimated. According to Lau (1981), the RMS amplitude of 500 mb monthly mean heights is $\sim$ 70% - 80% of that observed in the atmosphere.

They have not presented results of interannual variability of seasonal means.

b) Figure 12a shows the zonal means of observed and simulated standard deviation of daily and monthly mean 1000 mb geopotential height (m) for the Dec-Jan-Feb season. The model systematically underestimates the observed variability in the tropics. As the averaging period increases from one day to one month, the model simulated tropical variability decreases further. For example, at the equator, the model variability is $\sim$ 70% of the daily and only $\sim$ 45% monthly observed variability. Although this paper does not present any details of the variability of seasonal means, it can be argued that most of the monthly variability is due to the sampling of daily values which have rather large decay time of 4-8 days (see Figure 5.13 of Manabe and Hahn, 1981) and in much the same way, if the interannual variability of simulated seasonal means were calculated for the tropics it would also most likely be too low.

c) Figure 12b shows latitude - pressure distributions of zonal mean standard deviation of monthly mean geopotential height (m) for the Dec-Jan-Feb season. It is seen that although the extratropical variability is underestimated only slightly, the simulated tropical variability in the upper troposphere and stratosphere is smaller by factors of two or three, respectively.

d) The ratio of the observed to simulated standard deviation of Northern Hemisphere mean surface air temperature is about 1.8 for daily, 2.0 for three month running means and about 3.0 for twelve month running means. It is not clear if this difference is genuine or just due to differences in sampling of observed and model simulated data.

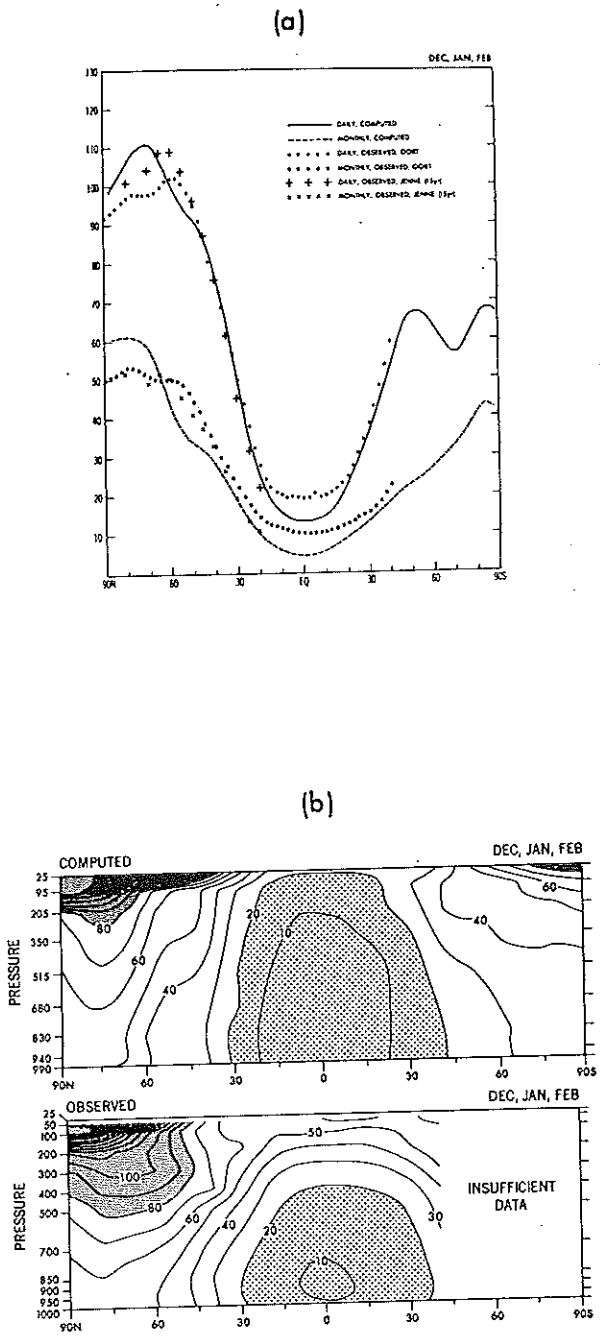

Figure 12 Zonal means of standard deviation for December-January-February season: (a) daily and monthly mean 1000 mb geopotential height, (b) latitude-pressure distribution for monthly mean geopotential height (m). Observations in (a) from Jenne and Oort, in (b) from Oort. (Manabe and Hahn, 1981).

e) The first eigenvector of the normalized monthly mean 500 mb height field for winter looks similar to the corresponding eigenvector for observations, although there are some differences in the locations and amplitudes of anomaly centres. The model simulated first eigenvector explains 22.4% of the hemispherically integrated variance.

This shows that even in the absence of variable SST anomalies, basic large scale fluctuations do occur in the model atmosphere. The basic mechanisms for such fluctuations are not clearly understood. They could be due to the interactions of fluctuating zonal winds with orography, to instability of the three dimensional flow, or to tropical and mid-latitude transient diabatic heat sources associated with episodes of enhanced/reduced precipitation caused by internal dynamics itself. A more detailed analysis of the model simulated rainfall is needed to investigate the possible role of tropical heat sources in causing these large scale fluctuations.

f) Figure 13 shows the structure of the first eigenvector of the normalized monthly mean geopotential height at (a) 300 and (b) 1000 mb, for all 12 months of the year over the tropics. The most conspicuous feature is the lack of zonal variation and complete absence of any signature of Southern Oscillation (not shown) which shows opposite polarity over the Indian Ocean and the eastern tropical Pacific. According to Lau (1981) the pattern based on winter data alone is very similar to the one shown here, and the next few eigenvectors do not show any signature of the Southern Oscillation.

Shukla (1981a) carried out 60 day integrations of the GLAS climate model with nine different initial conditions but identical boundary conditions. Three of these initial conditions were the observed atmospheric conditions of 1 January 1975, 1976 and 1977, and other six initial conditions were obtained by superimposing over the observed initial conditions a random perturbation for which the root mean square error for all the grid points was 3 m/s in u and v components of wind. Figure 14b shows the global map of standard deviation among nine monthly means for the second month (February) of the model integration. Figure 14a shows the standard deviation among observed monthly mean sea level pressure for 16 years (1961-76) for Godbole and Shukla (1981). The model simulated variability is uniformly smaller than the observed variability. This difference is partly due to absence of anomalous boundary forcings and partly due to the limited duration of the model integrations which do not allow very low frequency internal dynamics processes to affect the monthly means. Figure 15a shows the ratio of the zonally averaged observed to simulated standard deviations. The ratio is about two in the low latitudes and about one in the middle latitudes. Figure 15b shows the zonally averaged daily standard deviation of sea level pressure for observations and model simulations. There is good agreement between the simulated and observed daily standard deviations.

Figure 16b shows the standard deviation of model simulated monthly mean rainfall for February and Figure 16a shows the observed standard deviation of mean rainfall for the winter season over land for 16 years (1963-76). Although the general patterns of simulated standard deviations (large maxima and minima) show some similarity to the observations, the magnitudes, especially in the tropics, are grossly underestimated. This points out the great importance of the interannual variability of boundary forcings in affecting the interannual variability of monthly and seasonal mean rainfall.

Charney and Shukla (1981) examined the variability of the monthly mean (July) circulation for four model runs for which the boundary conditions were kept identical but the initial conditions were randomly perturbed. It was found that although the observed and model variabilities were comparable at

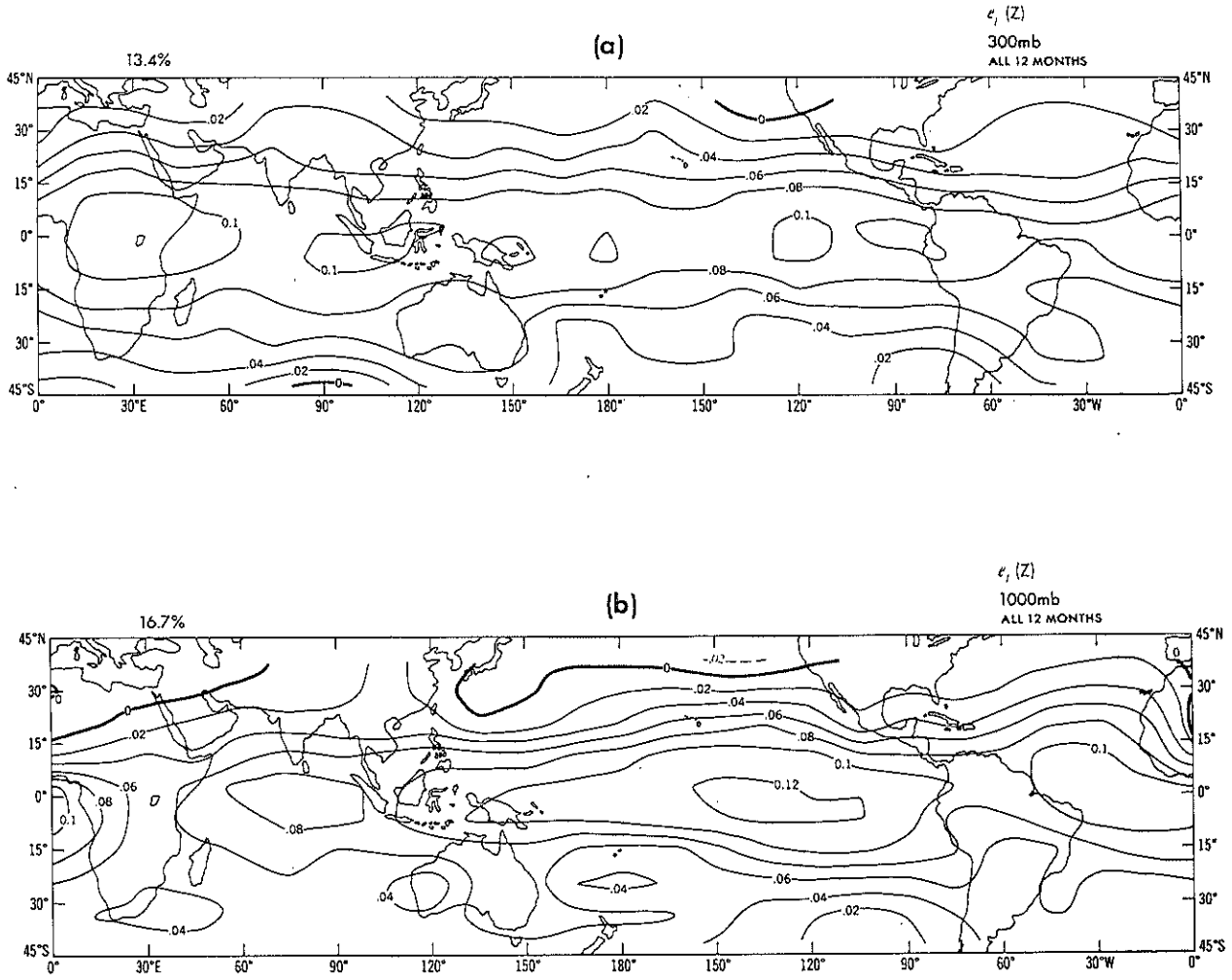

Figure 13 Distributions of the eigenvectors associated with the first principal component of normalized monthly mean geopotential height at (a) 300 mb and (b) 1000 mb for all 12 months of the year over the tropics (Lau, 1981).

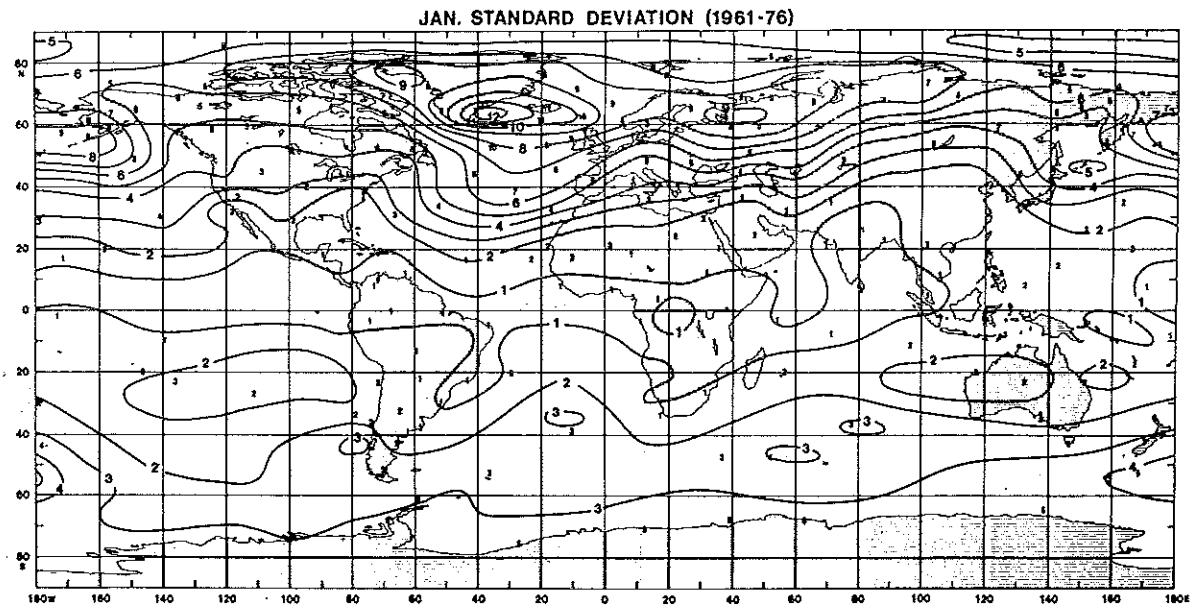

(b)

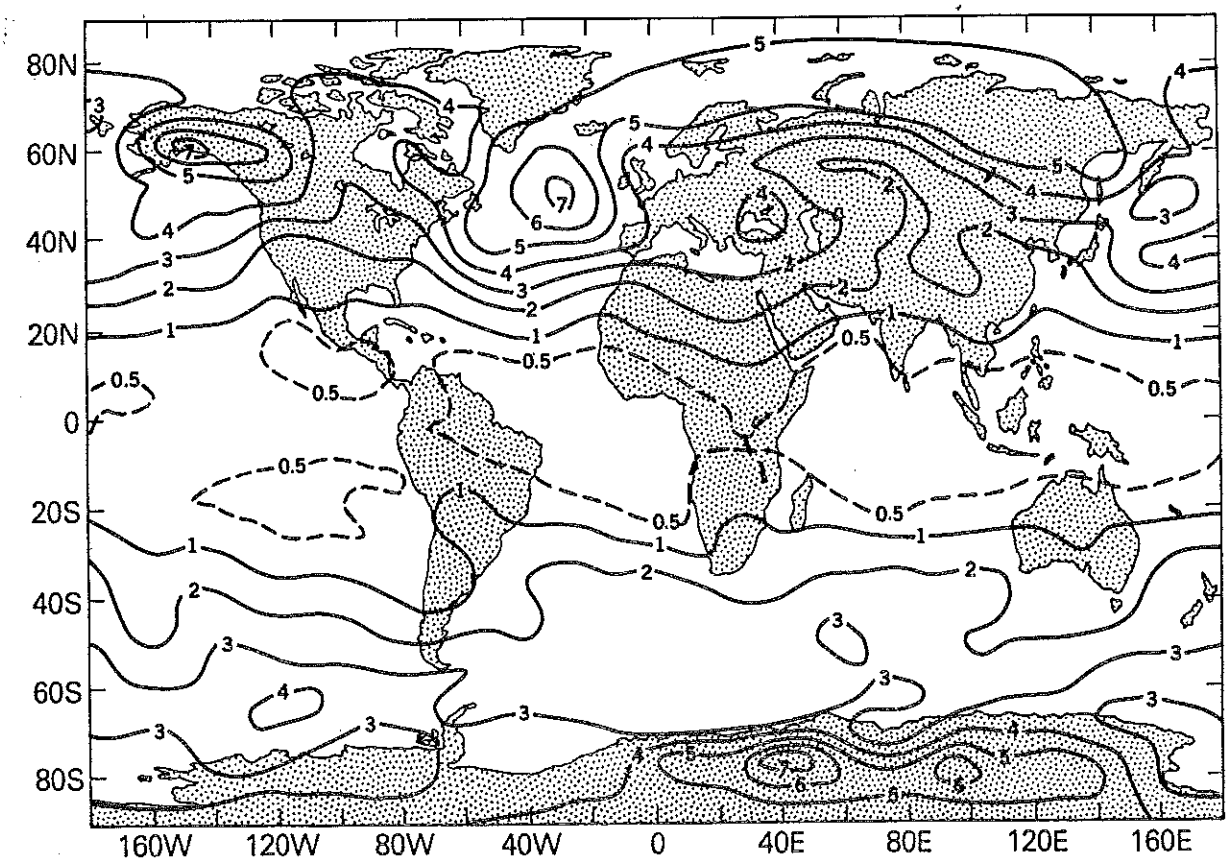

Figure 14 Standard deviation of monthly mean sea level pressure: (a) observed January (Godbole and Shukla, 1981), (b) GCM February (Shukla, 1981a).

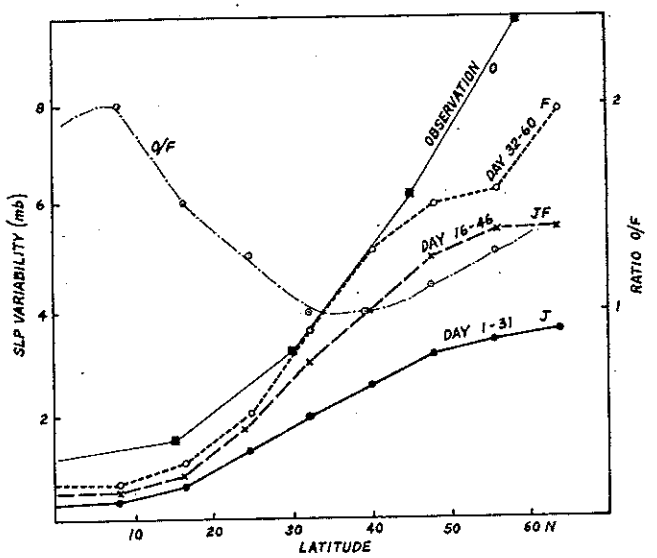

(b)

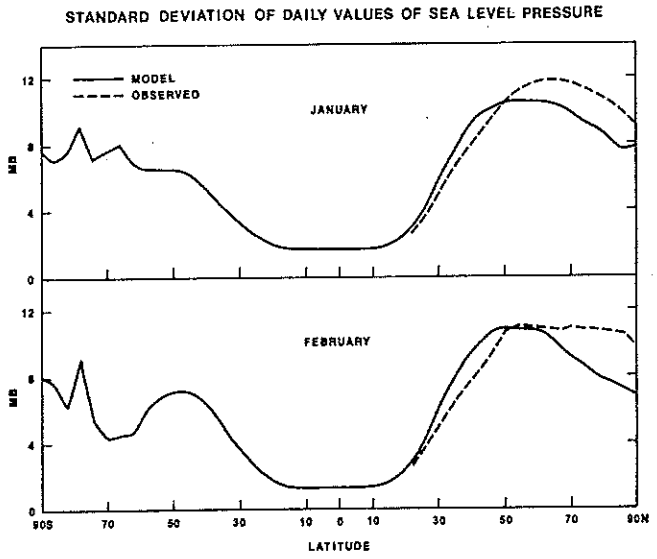

Figure 15 (a) Zonally averaged rms deviation between control and perturbation runs averaged for days 1-31, 16-46, and 32-60. O/F is ratio of observations and model days 32-60 (Shukla, 1981a).

(b) Zonally averaged standard deviation of daily grid point values for sea level pressure for January (upper panel) and February (lower panel) for model (solid line) and observations (dashed line). (Shukla, 1981a)

(a)

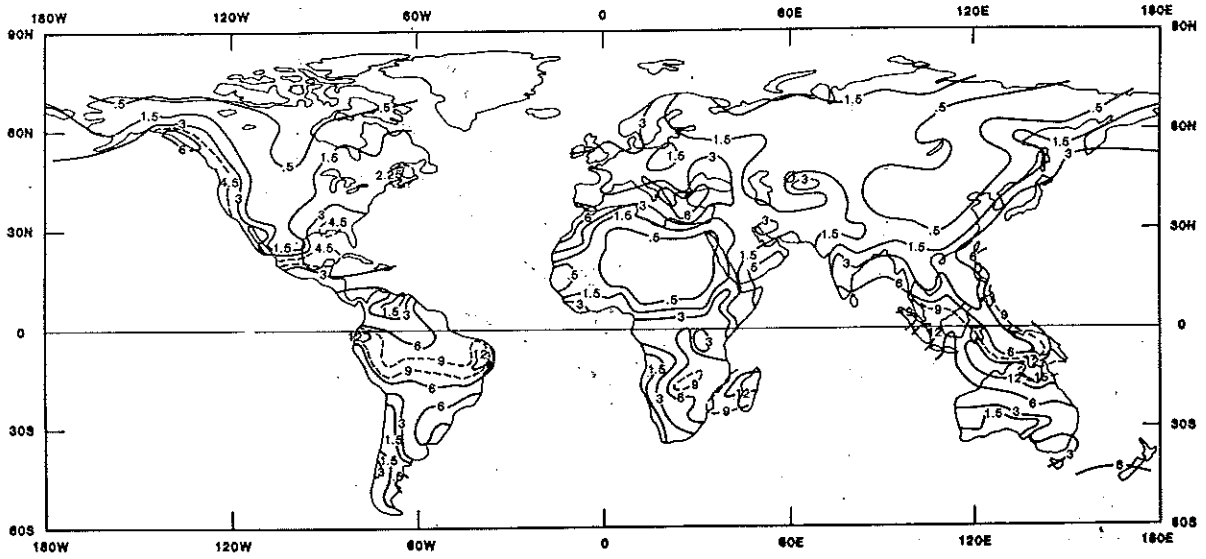

(b)

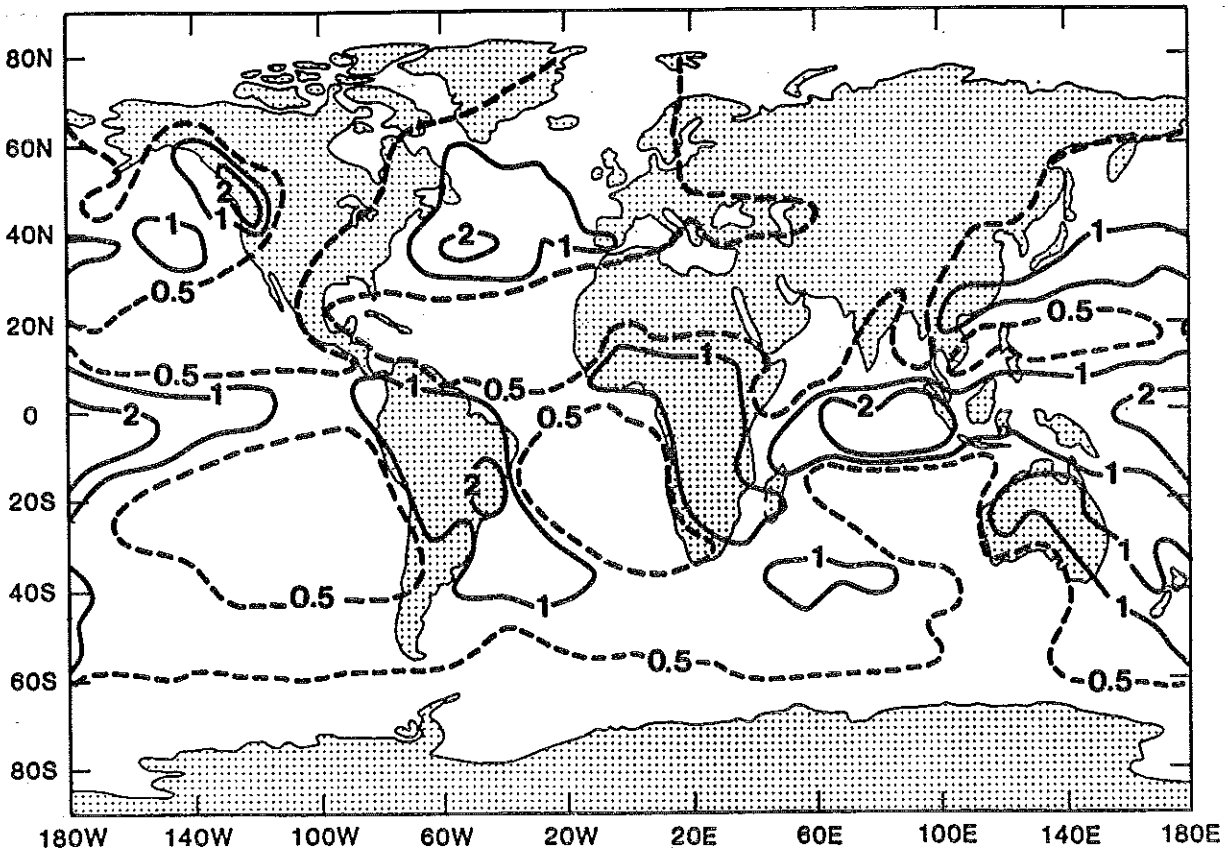

Figure 16 Standard deviation of (a) observed seasonal mean rainfall based on 16 years (1962-77), (b) GCM February mean rainfall for nine model runs (Shukla, 1981).

middle and high latitudes, the variability among the four model runs for the monsoon region was far less that the observed interannual variability of the atmosphere. From this it was concluded that the remaining variability could be due to the influence of boundary conditions. Similar conclusion has been drawn by Manabe and Hahn (1981) to explain the model simulated low variability in the tropics. A possible limitation in drawing such conclusions about the role of boundary forcings from these experiments arises because the model simulations were compared directly to observations. It would be more appropriate to make two integrations, one with and the other without the influence of the boundary forcings, so that two properties of the same model can be directly compared and any intrinsic model deficiency will not bias the results. A preliminary study along these lines has been carried out by Shukla (1981b) and the results are summarized below.

We carried out a 45-day integration of the GLAS climate model starting from the observed initial conditions in the middle of June and climatological mean boundary conditions. This integration is to be referred as control (C) run. For identical boundary conditions three additional integrations were carried out for 45 days by randomly changing the initial conditions of u and v at each of the nine model levels. The random errors corresponded to a Gaussian distribution with zero mean and standard deviation of 3 m/s for u and v separately. These integrations are to be referred to as Predictability (P_1, P_2, P_3) runs. Three additional integrations were carried out for 45 days, in which, in addition to randomly perturbed initial conditions, the boundary conditions of SST between equator and 30°N were replaced by the observed SST during July of 1972, 1973, 1974. These integrations are to be referred as Boundary forcing (B_1, B_2, B_3) runs. The variance $(\sigma_p)^2$ among monthly means of C, P_1, P_2, P_3 give a measure of the natural variability of the model, i.e. variability caused by internal dynamics alone. The variation $(\sigma_B)^2$ among monthly means of Cl, B_1, B_2, B_3 give a measure of the variability due to boundary forcings of SST. We have compared σ_p and σ_B with the observed (σ_o) standard deviation for ten years of monthly means. Figure 17 shows the global maps of σ_o and σ_p. The July standard deviation fields for the model is considerably smaller than is observed, with the most pronounced discrepancy occurring in the tropics.

Figure 18a shows plots of zonally averaged values of σ_p, σ_B, σ_o and the ratios σ_o/σ_p and σ_o/σ_B. It is seen that in agreement with the results of Charney and Shukla (and Manabe and Hahn), the ration σ_o/σ_p is more than two in the tropics and close to one in the middle latitudes. The new result of this study is that the ratio σ_B lies nearly halfway between σ_o and σ_p which suggests that nearly half of the remaining variability was accounted for by changes in SST between equator and 30°N. The influence of other boundary forcings due to soil moisture or snow cover will further bring σ_B closer to σ_o. Although this conclusion is drawn from short period integrations, the results show remarkable agreement with the results of Manabe and Hahn based on 15 years of model integration. We have calculated the ratio σ_o/σ_M (where σ_M refers to model simulated standard deviations) from the two curves of Manabe and Hahn (shown in Figure 12a of this paper) and the results are shown in Figure 18b. It is again seen that the ratio (σ_o/σ_M) is about two in the near equatorial regions and is reduced to about one in the middle and high latitudes. The corresponding ratio is more than three (see Figure 12b) for the height field in the tropical troposphere and stratosphere.

These results, taken together with the analysis of Lau (1981) which showed that the Southern Oscillation was not simulated by the model simulations of Manabe and Hahn, indicate that the slowly varying boundary forcings are the most important mechanisms for determining the interannual variability

(a)

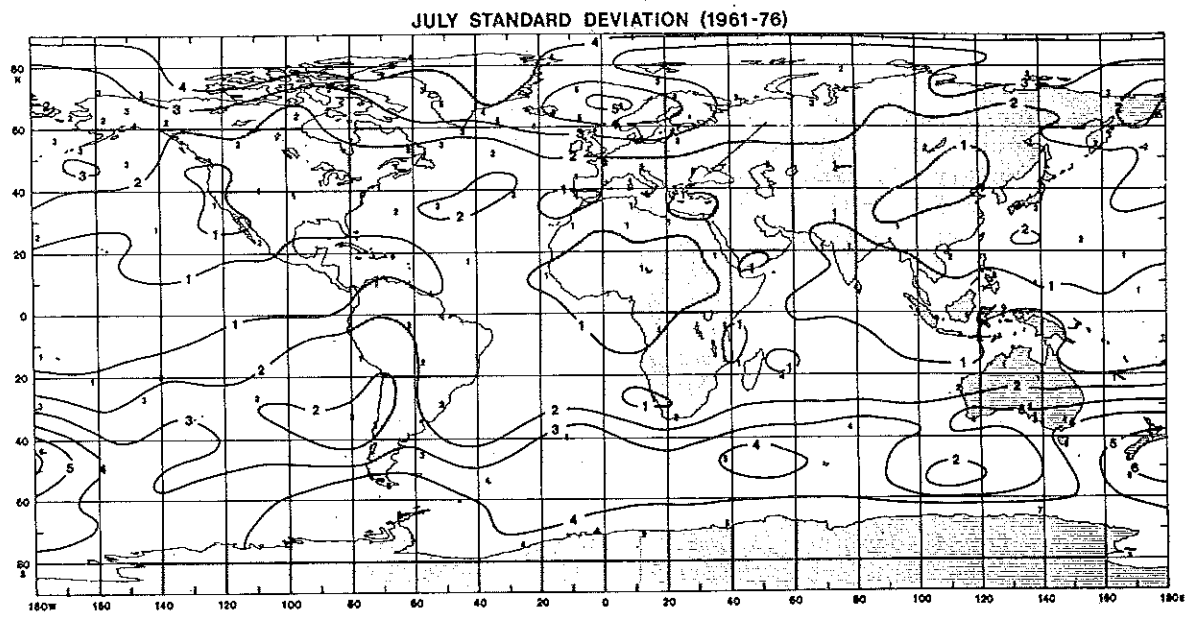

(b)

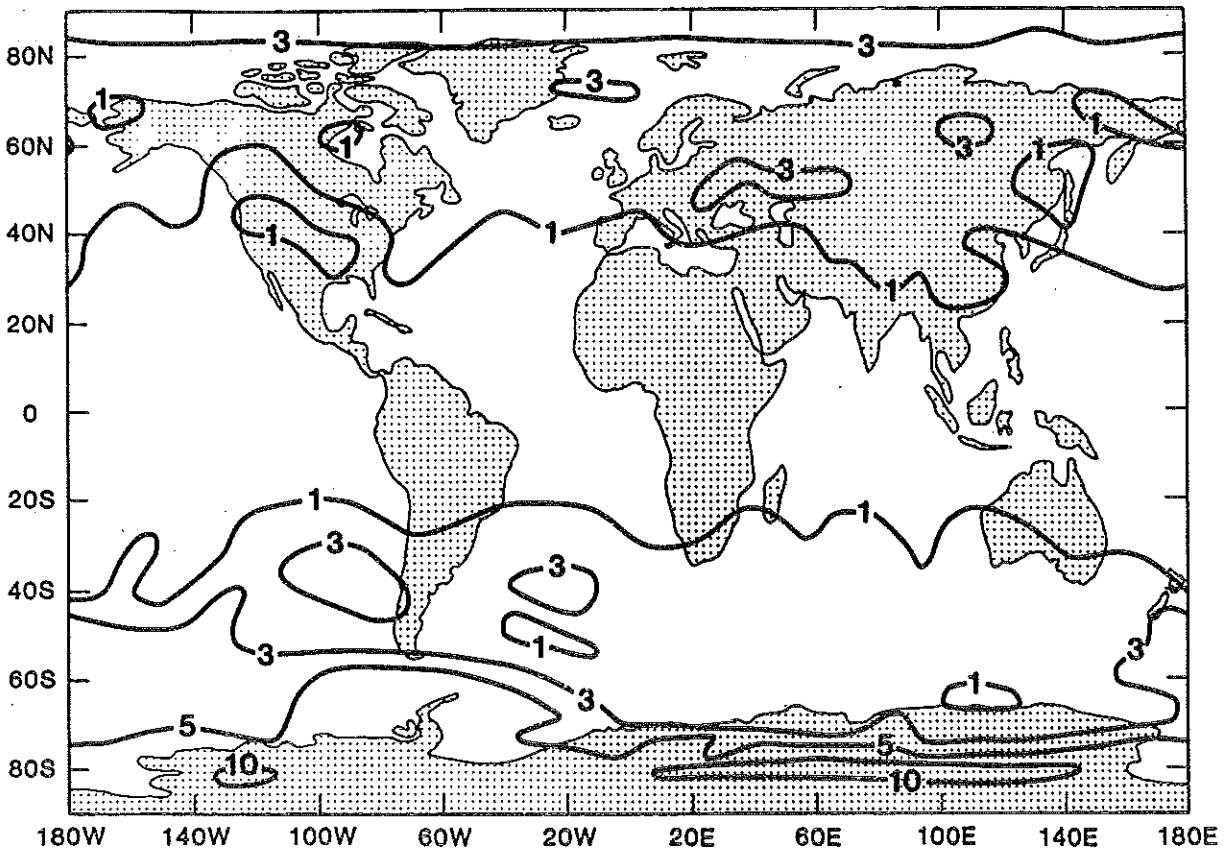

Figure 17 Standard deviation of monthly mean sea level pressure: (a) observed July (Godbole and Shukla, 1981), (b) GCM July (Shukla, 1981b).

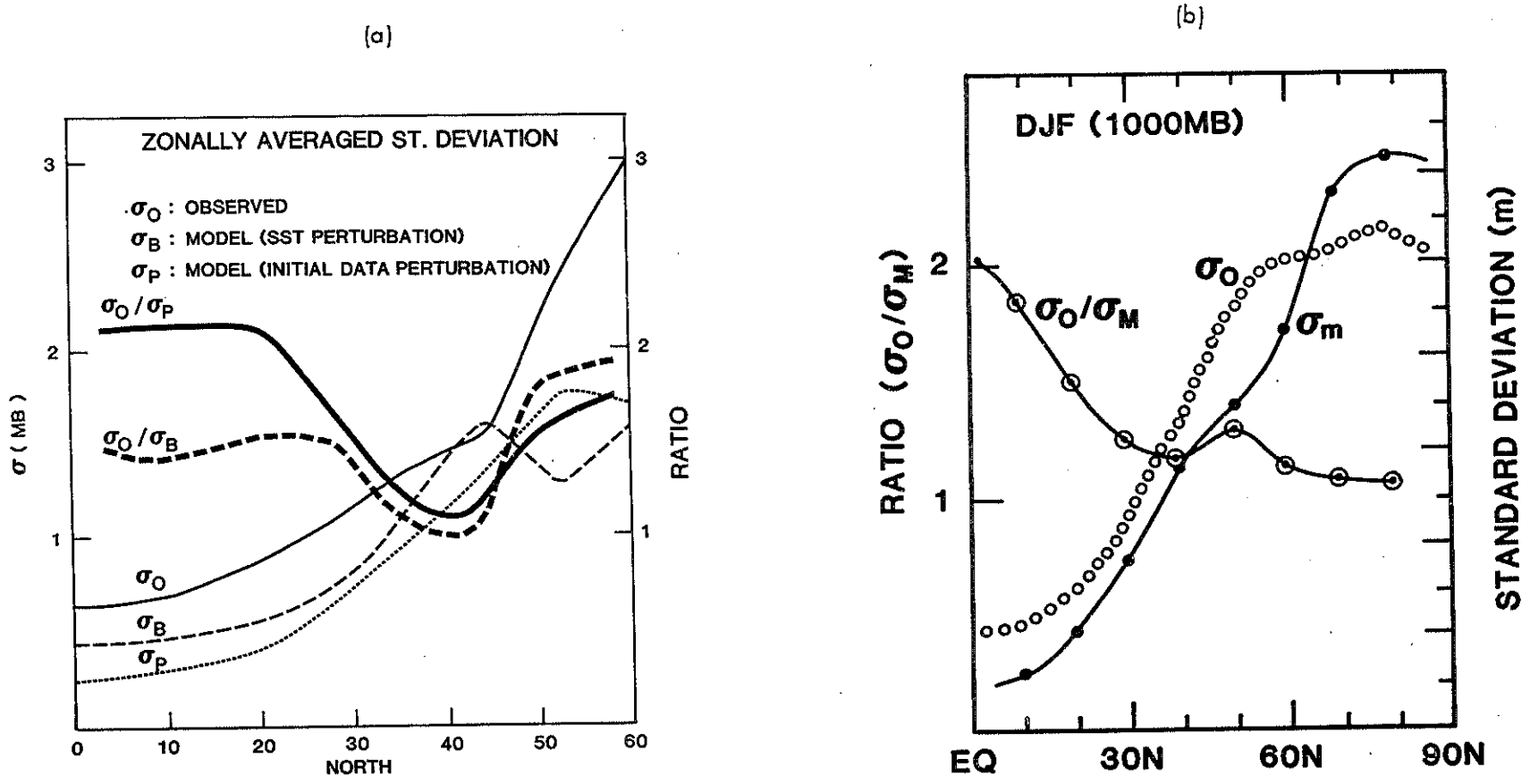

Figure 18 (a) Zonally averaged standard deviation among monthly mean (July) sea level pressure (mb) for 10 years of observations (σ_o, thin solid line); four model runs with variable boundary conditions (σ_B, thin dashed line); and four model runs with identical boundary conditions (σ_p, thin dotted line). Thick solid line and thick dashed line show the ratio σ_o/σ_p and σ_o/σ_B respectively.

(b) Zonal means of standard deviation of monthly mean 1000 mb geopotential height (m) from Manabe and Hahn (1981). On the left side is the ratio (σ_o/σ_m), of observed and model standard deviations.

of the monthly and seasonal means in the tropics. These are, however, indirect conclusions, and more systematic GCM simulation studies with and without boundary forcings are needed to understand the relative importance of internal dynamics and boundary forcings. It is not unlikely that the tropical boundary forcings also influence the simulation of the mid-latitude variability, but more model experiments are needed to provide a more definitive answer.

5. INTERANNUAL VARIABILITY OF INTRA-SEASONAL SPACE-TIME FLUCTUATIONS

To our knowledge no paper has yet appeared which describes the interannual variability of model simulated intra-seasonal space-time fluctuations. Figure 17 of Lau (1981) is the only result in this category that we could find. Lau has presented composite charts of RMS of band-pass filtered 500 mb height for simulated five winter seasons that had large positive amplitude of the first eigenvector of normalized monthly mean 500 mb height and compared it with a composite of another five winter seasons that had large negative amplitude of the same eigenvector. He found that the displacements of maxima of band-pass filtered RMS (which represent storm tracks) are consistent with shifts in large scale circulation features such as the location of jet streams and regions of enhanced baroclinicity.

6. SUMMARY AND CONCLUSIONS

a) Global multi-level atmospheric GCMs with prescribed climatological boundary forcings can realistically simulate the large scale circulation features of the observed summer and winter climatic means. Some systematic errors still remain to be removed.

b) Several model integrations have been carried out for the whole year or more to simulate the seasonal cycle. However, no detail analysis has yet been presented for the structure of the seasonal cycle itself (seasonal transitions, etc.) and all of the analysis is concerned with the individual seasons, mostly winter and summer.

c) Analysis of the space-time spectra of day to day fluctuations within a season have been carried out in great detail and compared with the observations. Most of the models show a remarkable degree of success in simulating the band-pass filtered variance and location, intensity, and duration of blocking events. Spatial structures of the co-variances (momentum and heat fluxes) for transient eddies are also simulated well.

d) Even with climatological boundary forcings, the interannual variability of monthly means in middle latitudes is simulated reasonably well but the simulated tropical variability is only half of the observed variability. It is reasonable to conclude, tentatively, that the internal dynamics are the most important mechanism for mid-latitude variability while boundary forcings are the most important mechanisms for the tropical variability. This conclusion is tentative because model integrations necessary to answer these questions have not been carried out yet and the analysis of existing model integrations is not complete enough. We cannot rule out the influence of mid-latitude and/or tropical boundary forcings in producing large circulation anomalies in mid-latitudes.

e) Interannual variability of model simulated day to day variability has not yet been examined.

ACKNOWLEDGEMENTS:

The author wishes to thank Dr. David Straus for reviewing the manuscript and making very useful suggestions, Mrs. Jody Reckley for excellent typing and Miss Debbie Boyer for helping with the figures.

REFERENCES:

Blackmon, M.L., J.M.Wallace, N.C.Lau and S.L.Mullen, 1977: An observational study of the Northern Hemisphere wintertime circulation. J.Atmos.Sci., 34, 1040-1053

Blackmon, M.L. and N.C.Lau, 1980: Regional characteristics of the Northern Hemisphere wintertime circulation: A comparison of the simulation of a GFDL general circulation model with observations. J.Atmos.Sci., 37, 497-514

Charney, J.G. and J.G.Devore, 1979: Multiple flow equilibria in the atmosphere and blocking. J.Atmos.Sci., 36, 1205-1216

Charney, J.G. and D.M.Straus, 1980: Form-drag instability, multiple equilibria and propagating planetary waves in baroclinic, orographically forced, planetary wave system. J.Atmos.Sci., 37, 1157-1176

Charney, J.G. and J.Shukla, 1980: Predictability of monsoons. Monsoon Dynamics, Cambridge University Press, Editors: Sir James Lighthill and R.P.Pearce.

Charney, J.G., J.Shukla and K.C.Mo, 1981: Comparison of barotropic blocking theory with observation. J.Atmos.Sci., 38, 762-779

Chen, T.C. and J.Shukla, 1981: Diagnostic analysis and spectral energetics of a blocking event in the GLAS climate model simulation. Submitted for publication to Mon. Wea. Rev.

Dole, R.M., 1982: Persistent anomalies of the extratropical Northern Hemisphere wintertime circulation. Ph.D.thesis. Mass. Inst. of Technology, Cambridge, Mass.

Gilchrist, A., 1982: Aspects of the simulation of climate and climate variability in middle latitudes. Study conference on the Physical basis for climate prediction on seasonal, annual and decadal time scale. Leningrad (USSR), 13-17 September 1982

Godbole, R.V. and J.Shukla, 1981: Global analysis of January and July Sea Level Pressure. NASA Tech. Memo. 82097

Halem, M., J.Shukla, Y.Mintz, M.L.Wu, R.Godbole, G.Herman and Y.Sud, 1979: Comparisons of observed seasonal climate features with a winter and summer numerical simulation produced by the GLAS general circulation model. GARP Publications Series No. 22, 207-253, WMO, Geneva, Switzerland

Hayashi, Y., 1974: Spectral analysis of tropical disturbances appearing in a GFDL general circulation model. J.Atmos.Sci., 31, 180-218

Hayashi, Y., 1980: Studies of the tropical general circulation with a global model of the atmosphere. Proc. of the seminar on impact of GATE on large-scale numerical modelling of the atmosphere and ocean, Woods Hole, Massachusetts, 20-29 August 1979, pp. 249-254 (National Academy of Sciences, Washington, D.C.)

Hayashi, Y. and D.G.Golder, 1980: The seasonal variation of tropical transient planetary waves appearing in a GFDL general circulation model. J.Atmos.Sci., 37, 705-716

Jaeger, L., 1976: Monatskarten des Niederschlags fur die ganze Erde. Berichte des Deutschen Wetterdienstes, 18, No. 139. Im Selbstverlag des Deutschen Welterdienstes, Offenbach, W.German.

Lau, N.C., 1981: A diagnostic study of recurrent meteorological anomalies appearing in a 15-year simulation with a GFDL general circulation model. Mon.Wea.Rev., 109, 2287-2311

Manabe, S. and J. Smagorinsky, 1967: Simulated climatology of a general circulation model with a hydrologic cycle. II. Analysis of the tropical atmosphere. Mon.Wea.Rev., 95, 155-169

Manabe, S., J.L.Holloway and H.M.Stone, 1970: Tropical circulation in a time-integration of a global model of the atmosphere. J.Atmos.Sci., 27, 580-613

Manabe, S., D.G.Hahn and J.L.Holloway, 1974: The seasonal variation of the tropical circulation as simulated by a global model of the atmosphere. J.Atmos.Sci., 31, 43-83

Manabe, S., D.G.Hahn and J.L.Holloway, 1979: Climate simulations with GFDL spectral models of the atmosphere: Effect of spectral truncation. GARP Publications Series No. 22, 41-94. (WMO, Geneva, Switzerland)

Manabe, S. and D.G.Hahn, 1981: Simulation of atmospheric variability. Mon. Wea.Rev., 109, 2260-2286

Mansfield, D.A., 1981: The incidence of blocking in the Meteorological Office's 5-level model. Met. O.13 Branch Memorandum No. 99, Meteorological Office, Bracknell

Mintz, Y. and G.Dean, 1952: The observed mean field of motion of the atmosphere. Geophys. Res. Papers, 17, 1-65

Sadler, J.C., 1975: The upper tropospheric circulation over the global tropics Department of Meteorology, University of Miami, Florida

Shukla, J., 1981a: Dynamical predictability of monthly means. J.Atmos. Sci., 38, 2547-2572

Shukla, J., 1981b: Predictability of the tropical atmosphere. NASA Tech. Memo No. 83829, pp. 1-51

Shukla, J., D.Straus, D.Randall, Y.Sud and L.Marx, 1981a: Winter and summer simulations with the GLAS climate model. NASA Tech. Memo. No. 83866, pp. 1-282

Shukla, J., K.C.Mo and M.Eaton, 1981b: Climatology of blocking in the GLAS climate model. NASA Tech. Memo.No. 83907, pp. 207-216

Shukla, J. and K.C.Mo, 1981: Seasonal and geographical variation of blocking. Submitted for publication to Mon.Wea.Rev.

Tung, K.K. and R.S.Lindzen, 1979: A theory of stationary longwaves. Part I. A simple theory of blocking. Mon.Wea.Rev., 107, 714-734.